"Road to Room Temperature Superconductivity",
Loen, Norway, June 17-23, 2007

Nanotechnology for Promise of RTS:
Search for Excitonic SC by combined SQUID/LFMA

Ali Aliev, Ray Baughman and
Anvar Zakhidov

Nanotech Institute

The University of Texas at Dallas

Outline

- Nanotechnology gain from HTS: discovery of single wall carbon nanotube by arc-synthesis
- Nano-system Zoo for RTS: dots, tubes, opals, inverted opals.
- Conventional LTS in nano-space: Pb inverted opal
- Inverse carbon opals: diamagnetism in NaxWO3 at 125 K , and in LixWO3-y at 132K
- Prospects: curved HTS and extra“excitonic pairing glue” across the interface in nanostructured SCs

Multi-walled

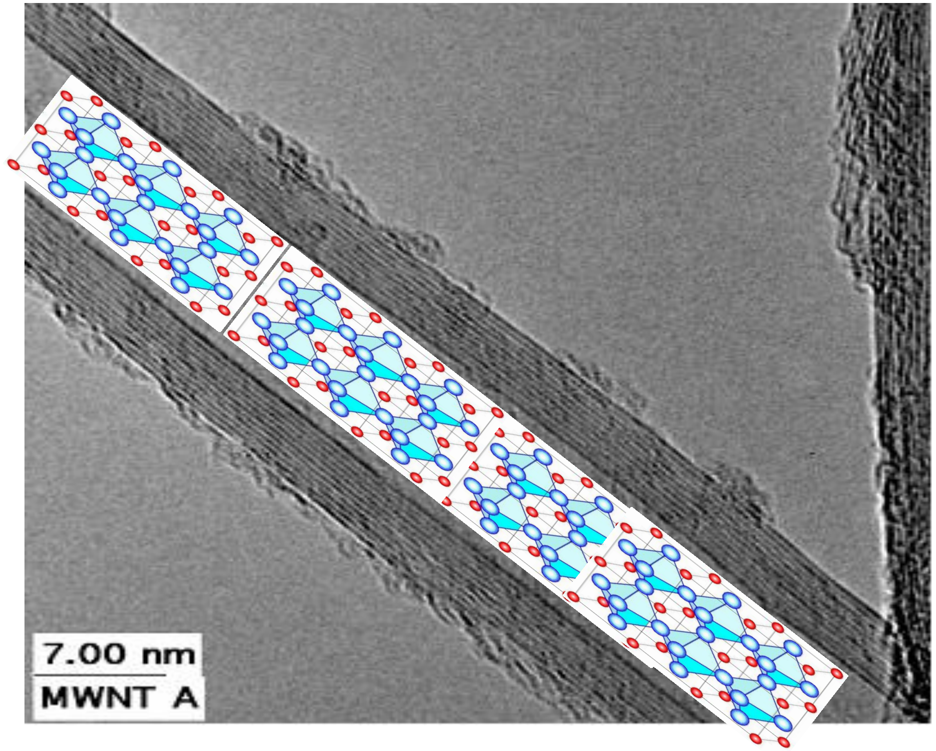

MWNT Cross-sectional view

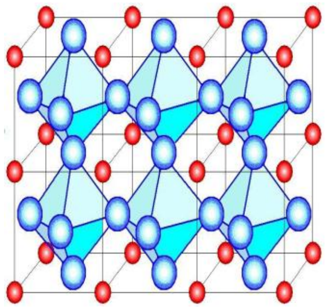

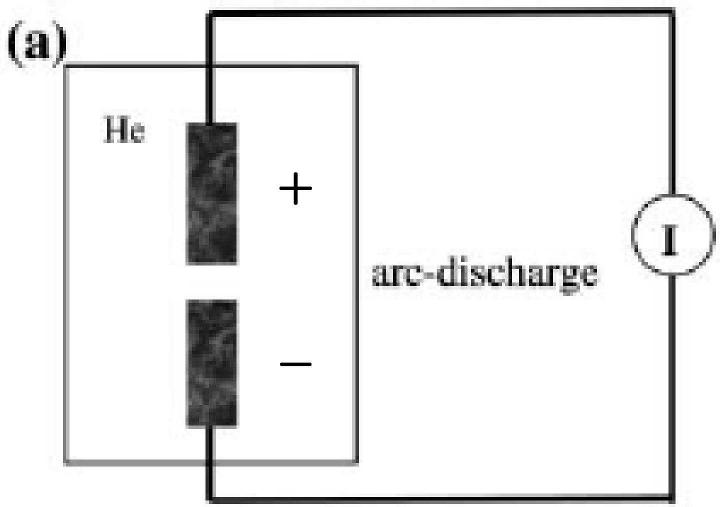

Ijima found MWCNTs at the cathode of arc discharge system.
For C60 synthesis
No catalyst was used

letters to nature

Large-scale production of single-walled carbon nanotubes by the electric-arc technique

C. Journet*, W. K. Maser*†, P. Bernier*, A. Loiseau‡, M. Lamy de la Chapelle§, S. Lefrant§, P. Deniard§, R. Lee‖ & J. E. Fischer‖

** Groupe de Dynamique des Phases Condensées, Université de Montpellier II, 34095 Montpellier cedex 5, France*
‡ LPS, ONERA, BP 72, 92322 Châtillon cedex, France
§ IMN, Université de Nantes, BP 32229, 44322 Nantes cedex 3, France
‖ LRSM, University of Pennsylvania, Philadelphia, Pennsylvania 19104-6272, USA

Single-walled

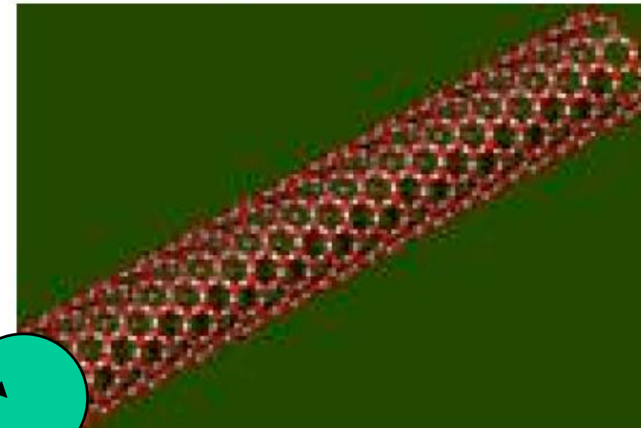

Y-catalyst cluster

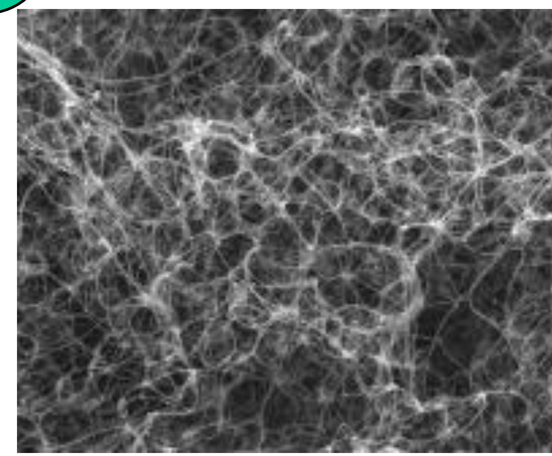

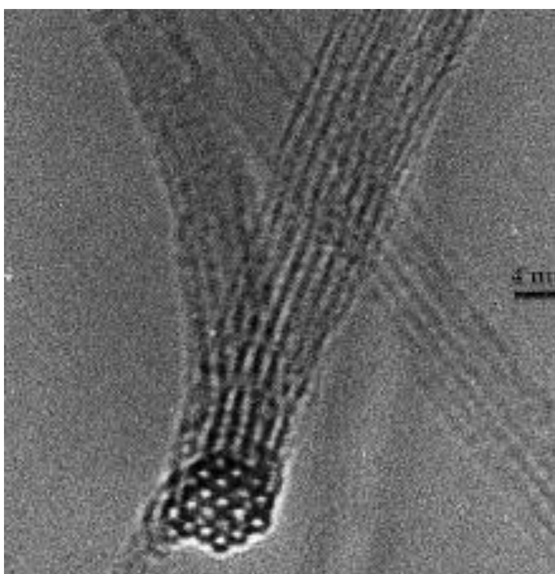

Bundle

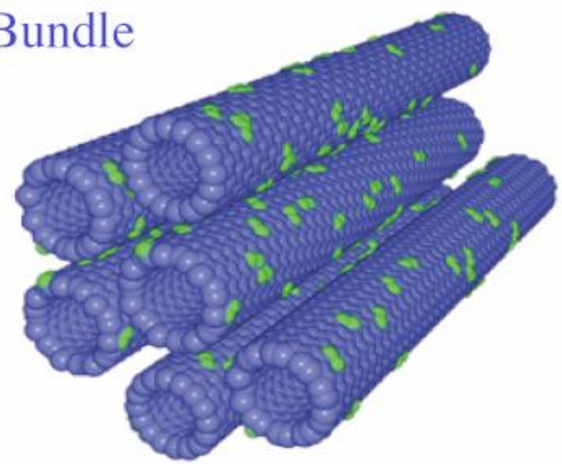

Used Y, Ba, Cu, O
In anode carbon rod with a hope to obtain MWCTS filled with 123 HTS

Description of CNT Tubes

Carbon nanotubes – quasi 1d structures with unique properties

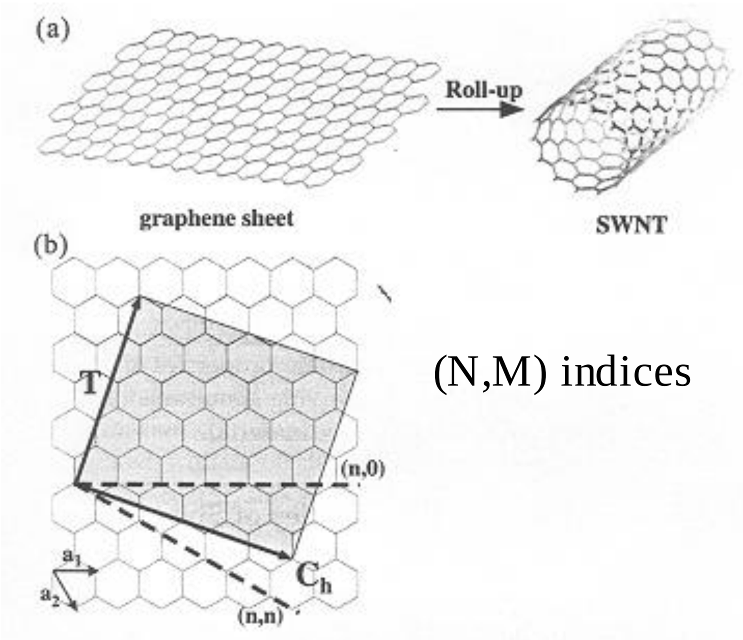

(N,M) indices

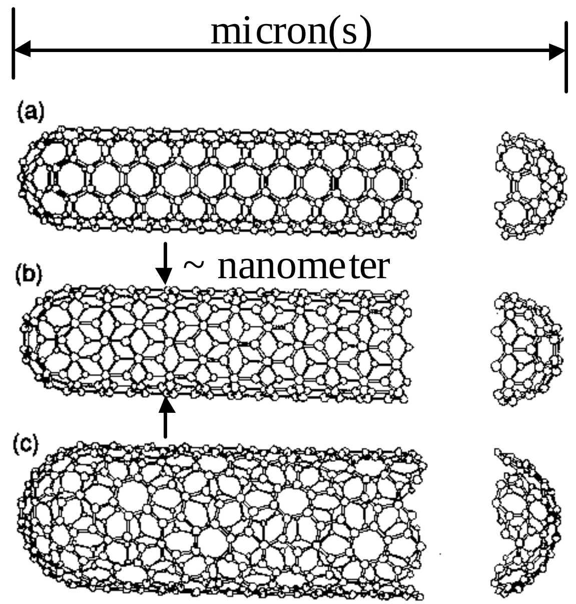

- Single wall NT
- Multiwall NT
- NT ropes
- NT mats…

- Armchair (5,5) tube - metal
- Zig-zag (9,0) tube – very small gap semiconductor (curvature effect)
- Chiral (10,5) tube - semiconductor

2-D layers of graphene at nanoscale self-curve into 0-D Dots, 1-D nanotubes, 3-D networks of inverted f.c.c.

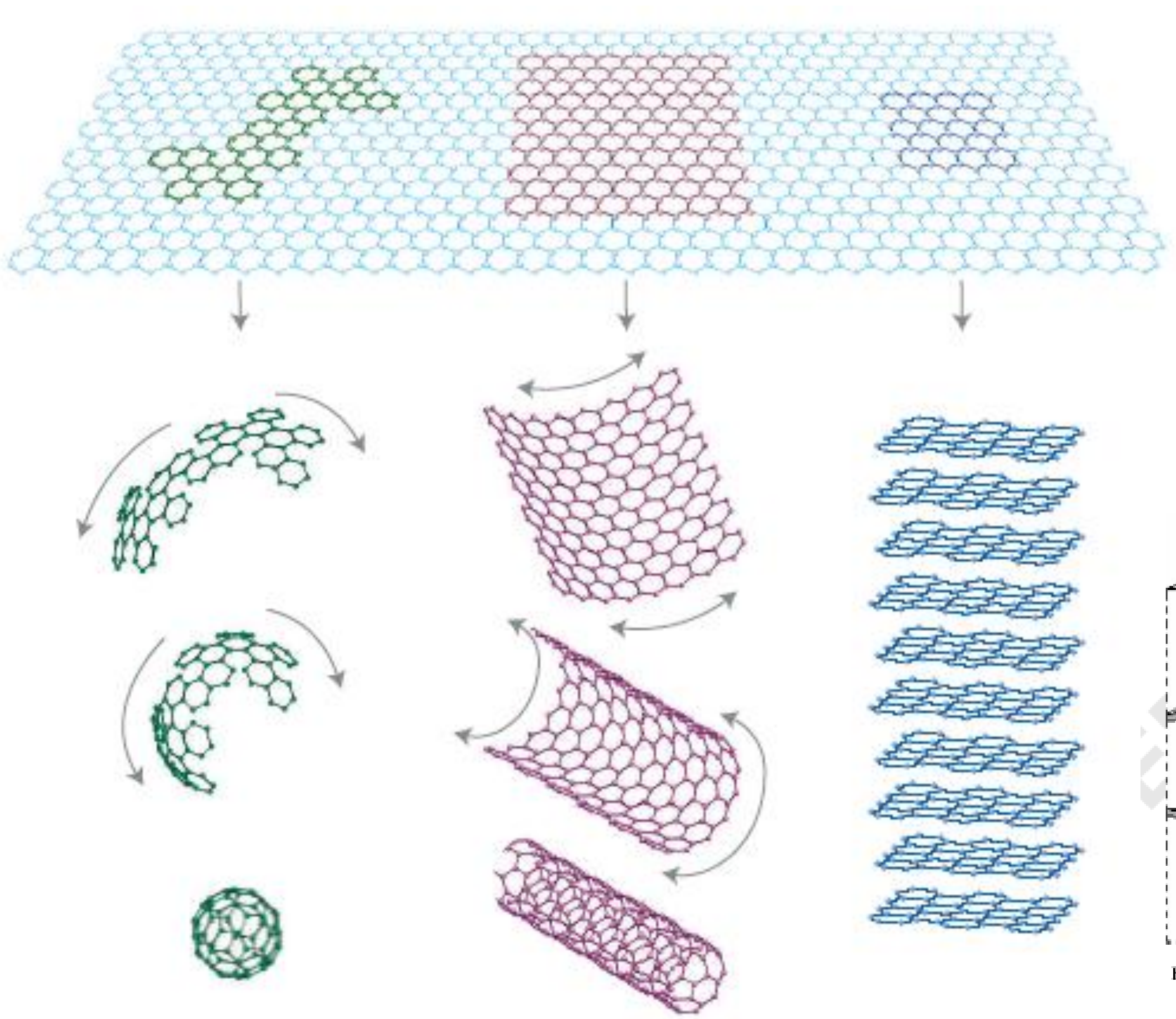

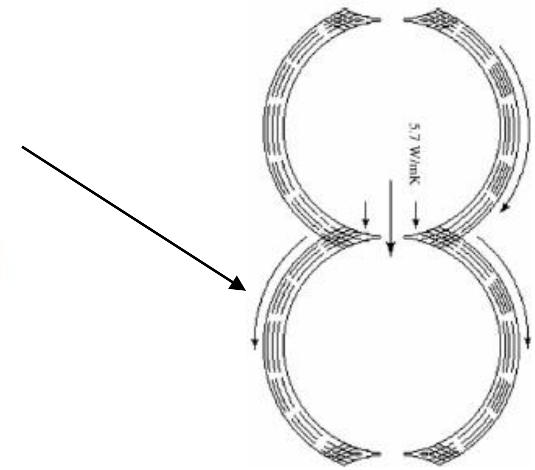

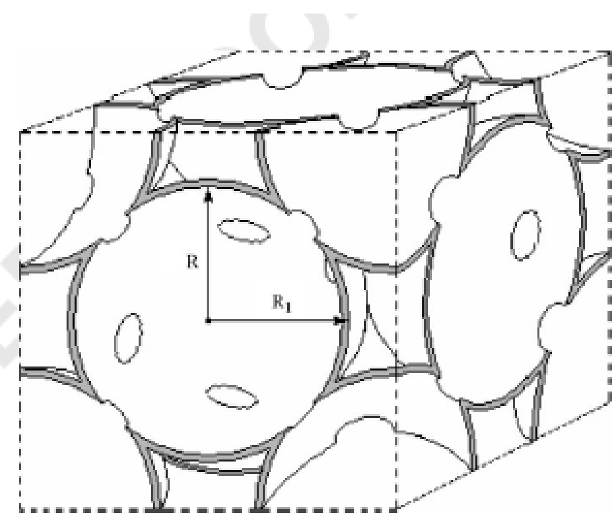

Fig. 3. Schematic representation of the surface-templated inverse opal.

NanoTemplates for Superconductors

Carbon Nanotubes

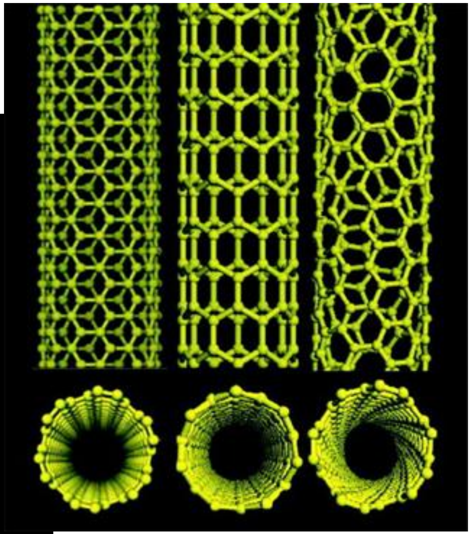

Can we create HTS materials at nanometer scale with Increased Tc, Hc, Isc, etc. via huge interface and curvature

Multiwall nanotubes

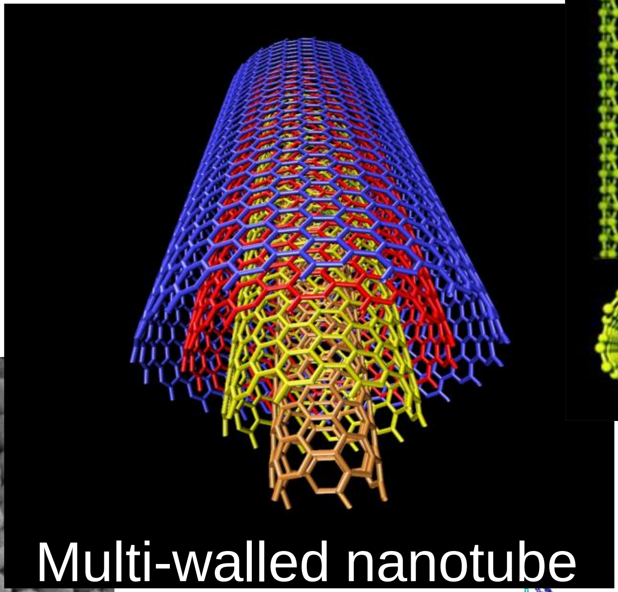

Opals

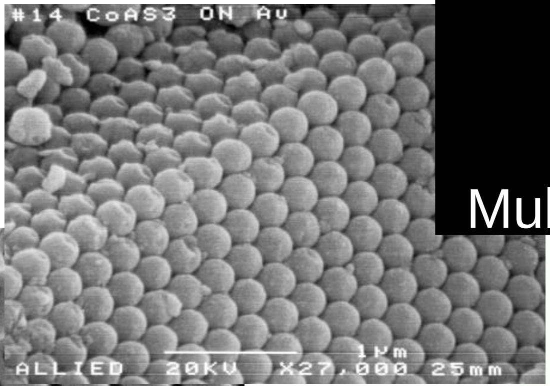

Inverted opals

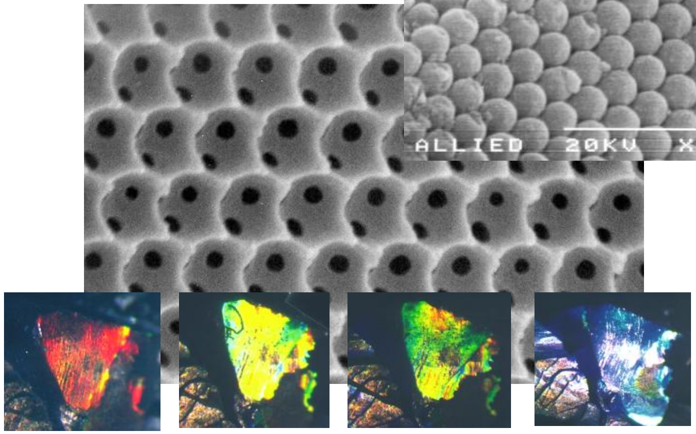

Transparent metallic nanofoams

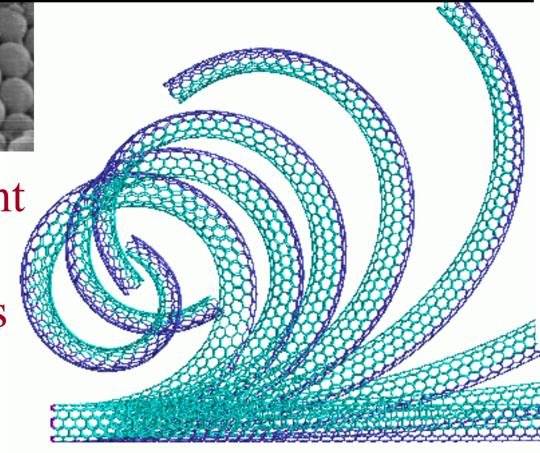

Double Layer Charge injection in nanotubes

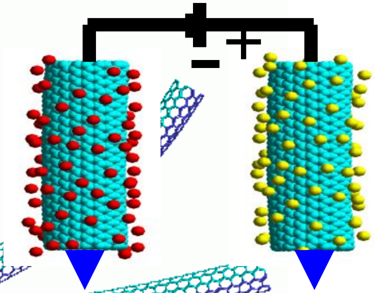

Force

Geometry for Opal-Derived FCC Structures

(111) Plane for Direct Opal

(100) Plane for Surface-Templated Inverse Opal

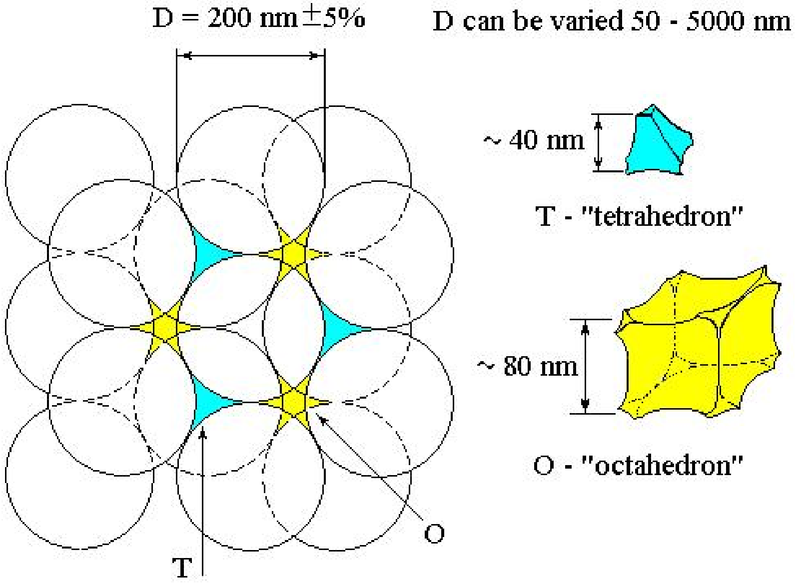

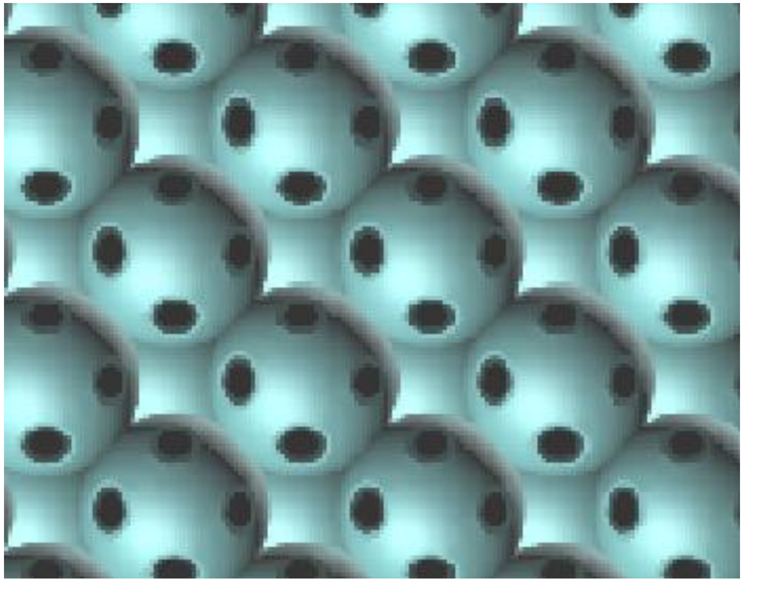

- Infiltration can either coat the internal surface or fill the internal volume.
- Template (SiO2 opal) cannot be infiltrated and then extracted unless <u>1.11 > d/D > 1.15,</u>
  d - intersphere separation, D - sphere diameter

Advantages of nano-space for growing HTS

Huge interface: >100 m2/cm3 accessible for SC growth.

Possibility to dope by “double layer charge” of ions at the surface

Possibility to self –assembled (SAM) layers of excitonic molecules

Curved surfaces: new phonon spectra

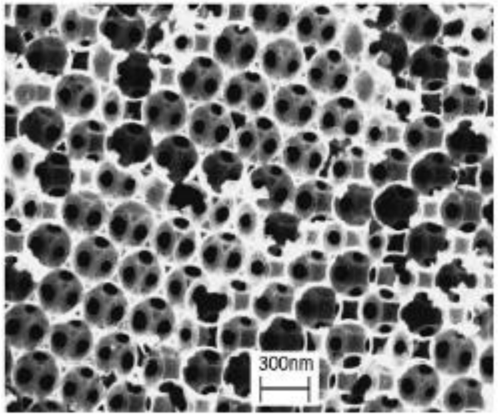

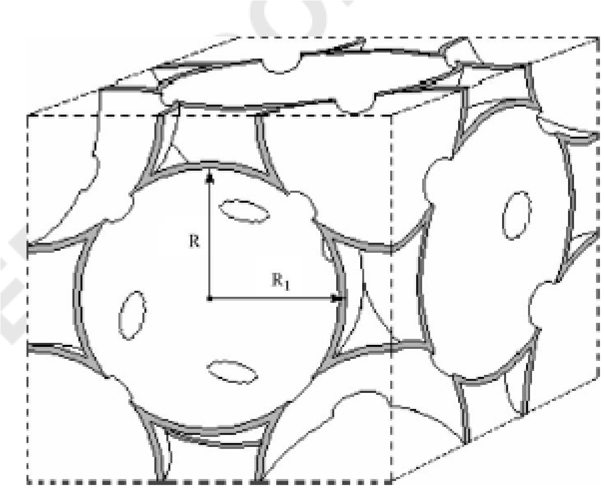

Fig. 3. Schematic representation of the surface-templated inverse opal.

Synthetic Opal:
Porous Silica Filled with Chloroform

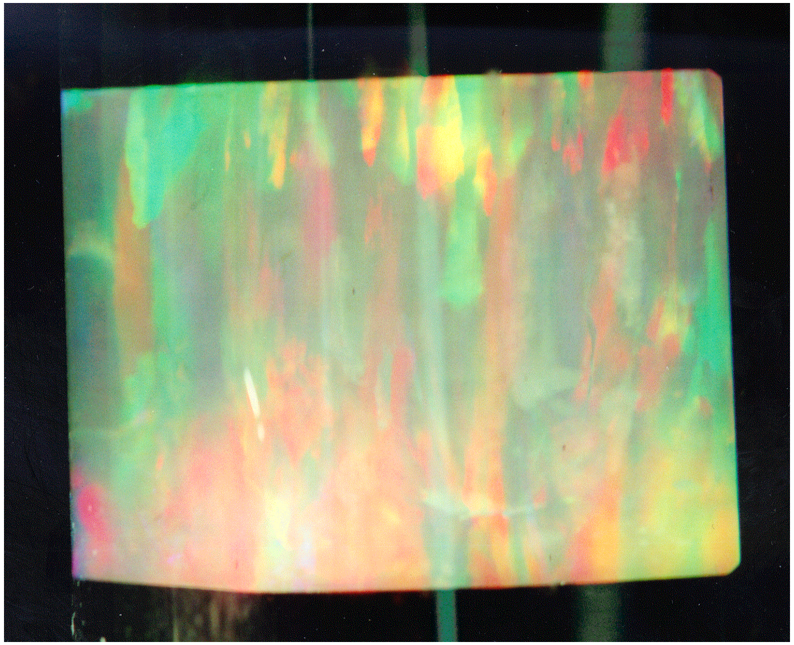

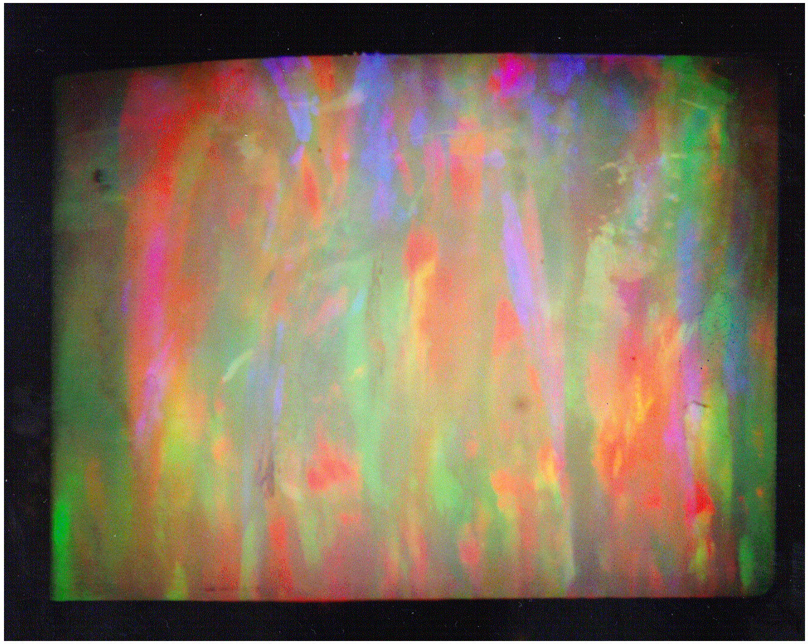

However the colors are not very bright, meaning PBG is not wide, since filling factor for air is small

Porous Opal Photonic Crystals

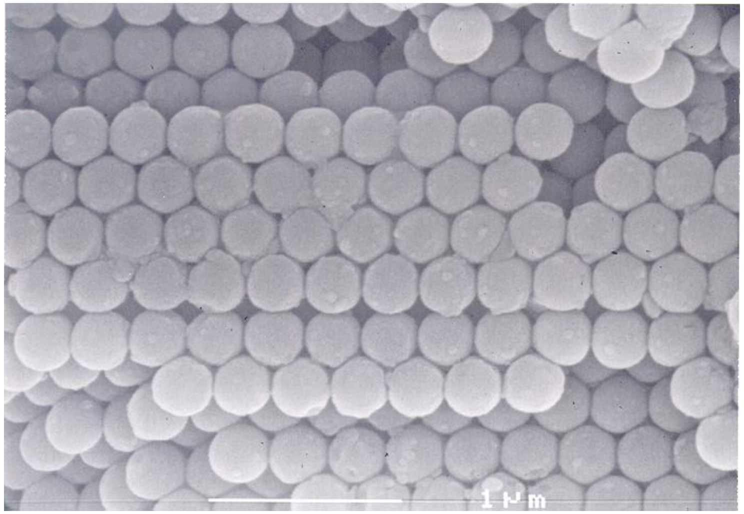

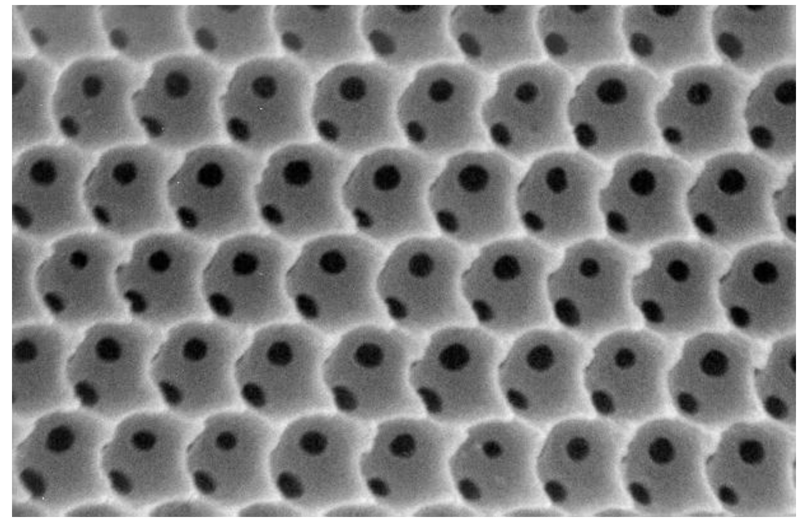

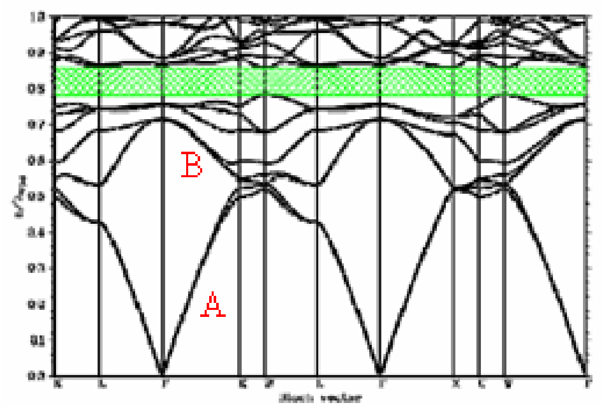

Huge internal porosity:
> 100 m2/cm3

There is a range of frequencies (green color) where light can not propagate

Inverse Opals Have > 75 % porosity

Science,
Vol. 282,
(1998),
p. 833

This inverted opal material
is a transparent polymer

Any material can be
Used for making
Inverted opals:
-Gold
-Diamond
-Carbon (conductive)
-Metals,
-semiconductors
-superconductors

Inverse Opals: Advantages for Templating of different materials

• Low filling factor ff< 0.24

• Can be made of any material:

•Metals, semiconductors,

•Lasing media: Er, Eu.

•Quantum dots

• Can infiltrate easily various materials with large change of (1-ff)

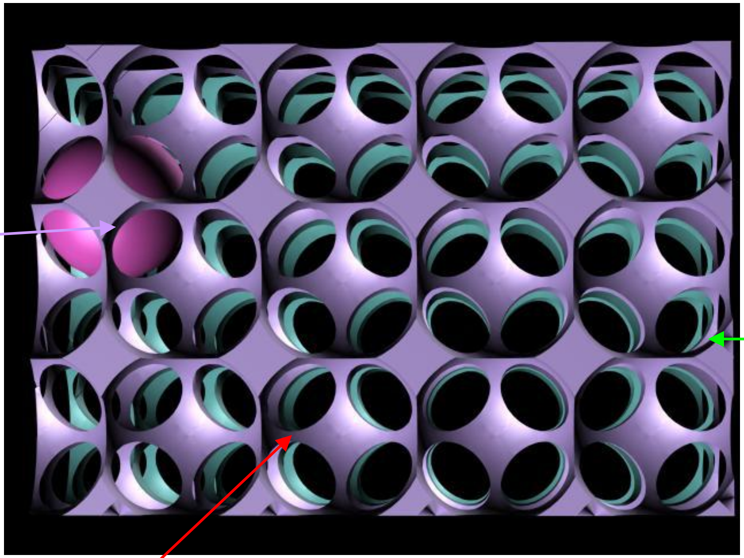

•Can change **n** by filling with transparent liquids

Can use electrochemistry, if the matrix is conductive

• Control connectivity between T and O via narrow necks: “network-cermet “transition: change of R and T

LTS in nanostructure: Pb-in-opal.
Will Tc, Hc, change for Pb clusters network

Available online at www.sciencedirect.com

ScienceDirect

Physica C 453 (2007) 15–23

PHYSICA C

www.elsevier.com/locate/physc

Superconductivity in Pb inverse opal

Ali E. Aliev *, Sergey B. Lee, Anvar A. Zakhidov, Ray H. Baughman

NanoTech Institute, University of Texas at Dallas, Richardson, TX 75083-0688, United States

Received 27 December 2005; received in revised form 14 October 2006; accepted 8 December 2006
Available online 22 December 2006

Fabrication of LTS: Pb Inverse Opal

1. POROUS SILICA OPAL

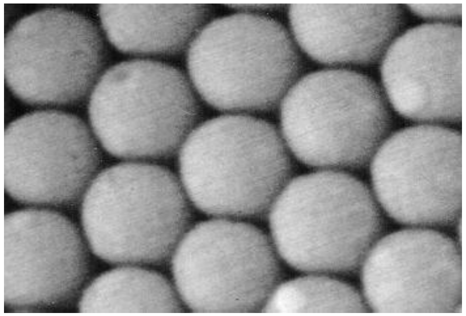

HIGH-PRESSURE
MELT-INFILTRATION

2. METAL-SILICA NANOCOMPOSITE

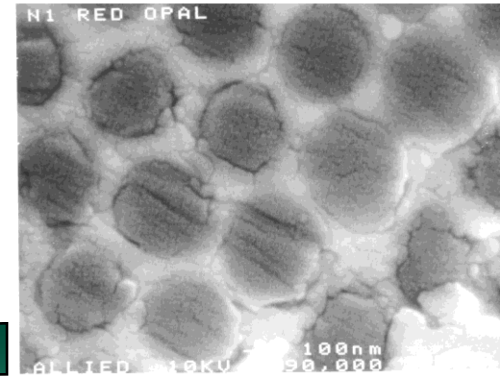

REMOVAL OF
SILICA WITH HF

3. METALLIC INVERSE OPAL

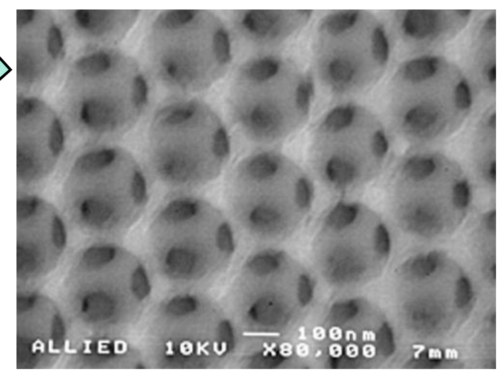

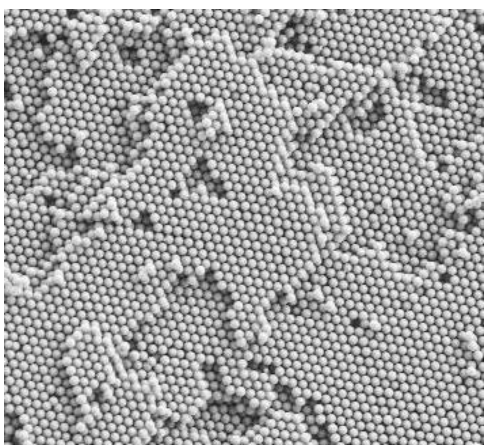

Structure of Pb-clusters network in pores of opal: Spheres connected via cylindrical channels

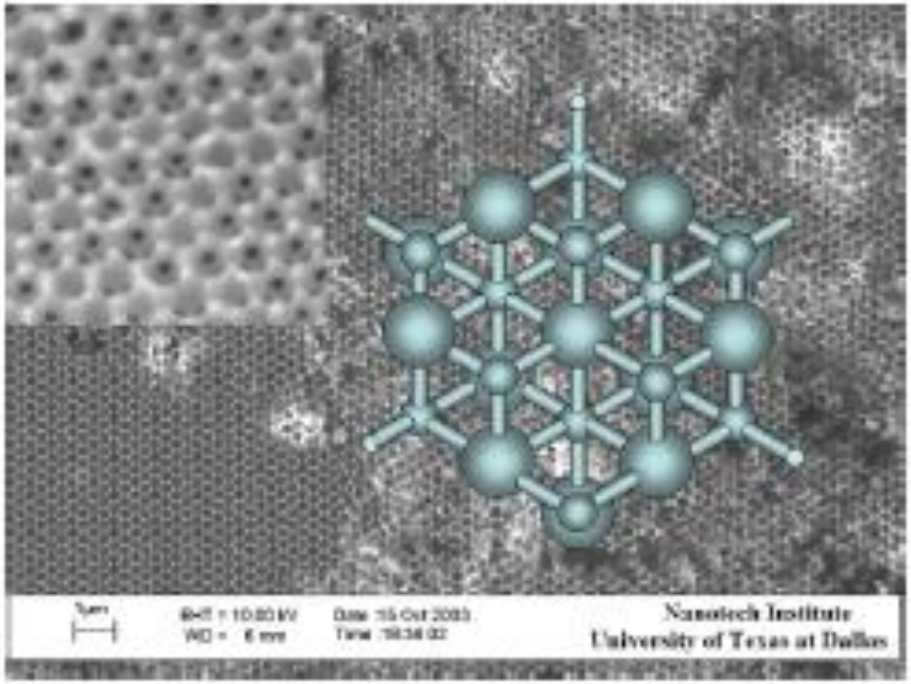

Fig. 1. SEM image of the (111) plane of the cleaved edge of a lead inverse opal. Highly crystalline structure is observable throughout the whole region. The top left corner inset shows a detail where the three channels in each void sphere connect with the spheres in the underlying layer. The void sphere diameter is 300 nm, which correspond to a red opal. The right inset shows a schematic representation of a lead inverse opal: octahedral and tetrahedral pores of fcc opal infiltrated with Pb can be represented as spheres ($r_o = 0.414 \cdot r$, $r_t = 0.225 \cdot r$) connected through cylindrical channels ($r_{ch} = 0.155 \cdot r$).

Table 1
Sample parameters

Parameter	Red inverse opal	Green inverse opal	Blue inverse opal	Bulk lead, Pb
Octahedral radius, nm	62.1	45.54	33.14	
Tetrahedral radius, nm	33.7	24.75	18.0	
Radius of channel, nm	23.2	17.05	12.4	
Weight, mg	24.8	24.8	24.8	211.88
Volume, mm^3	8.5	8.5	8.5	18.75
Density, g/cm^3	2.92	2.92	2.92	11.3

The radius of the lead infiltrated octahedral pores represented by big spheres in right inset to Fig. 1 is $r_o = R(\sqrt{2} - 1)$, the radius of tetrahedral pores is $r_t = R(\sqrt{3/2} - 1)$, and the radius of the interconnected channels is $r_{ch} = R(2/\sqrt{3} - 1)$. R is the radius of void spheres remaining after chemical extraction of silica spheres of direct opal.

Magnetization in red Pb opal (D=300 nm)
Tc increase from 7.1 K to 7.3 K, ΔTc = 0.3 K

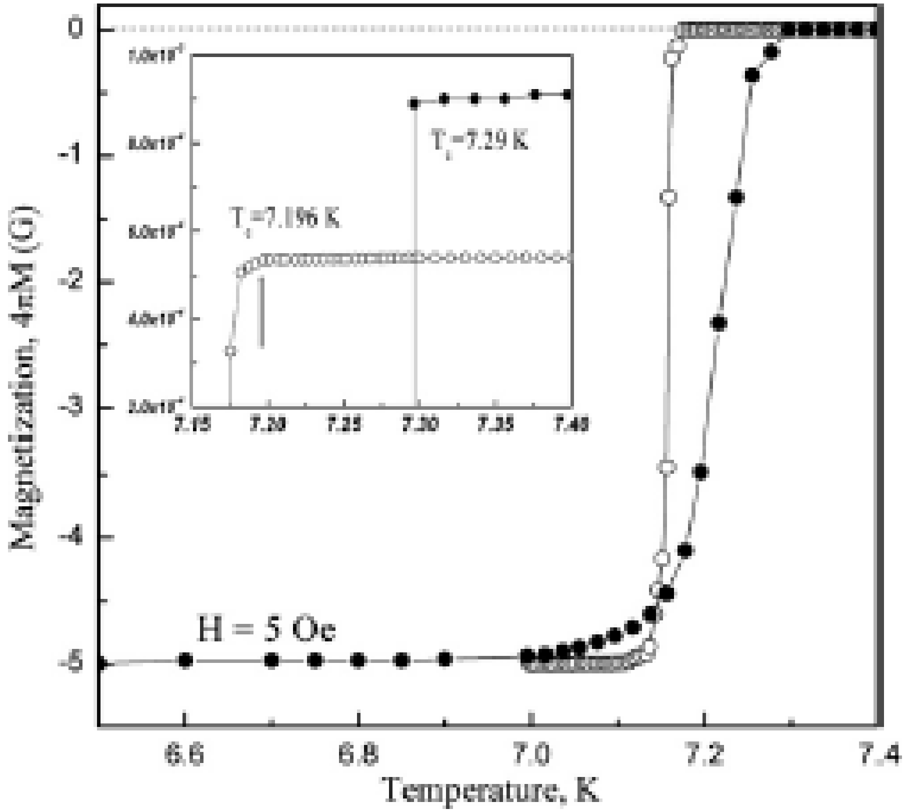

Fig. 2. The temperature dependences of ZFC magnetization for red Pb inverse opal (solid circles) and bulk Pb (open circles) at 5 Oe. The inset shows the ZFC magnetization near T_c.

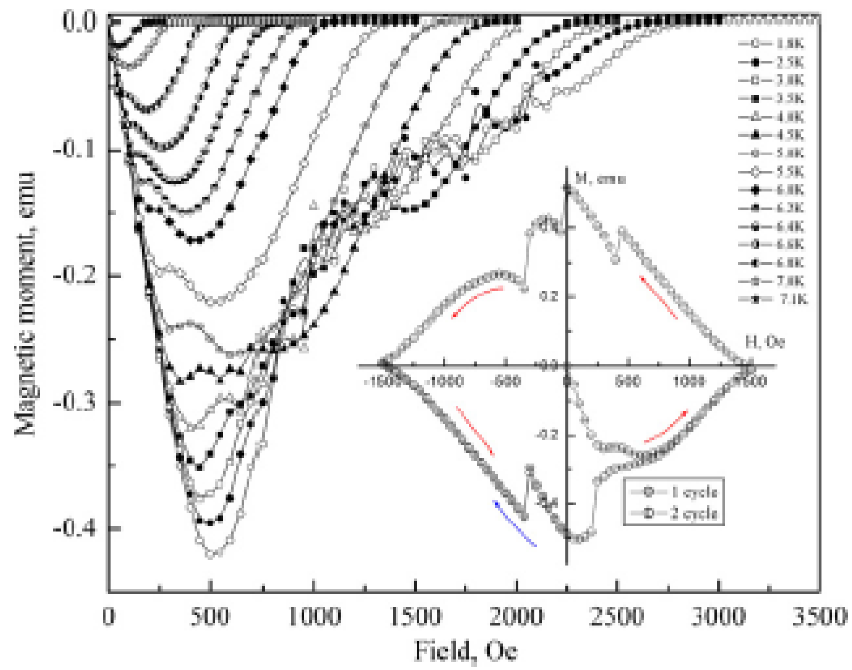

Fig. 4. Magnetization *vs.* external field for different temperatures. Two well-distinguished peaks have different behavior. Below 5 K the second maximum is dampened by the oscillation of the magnetic moment which disappears again at higher fields, $H > 0.8 H_{c2}$. The inset shows the whole

4-times Increase of critical Hc2 in Pb- opal

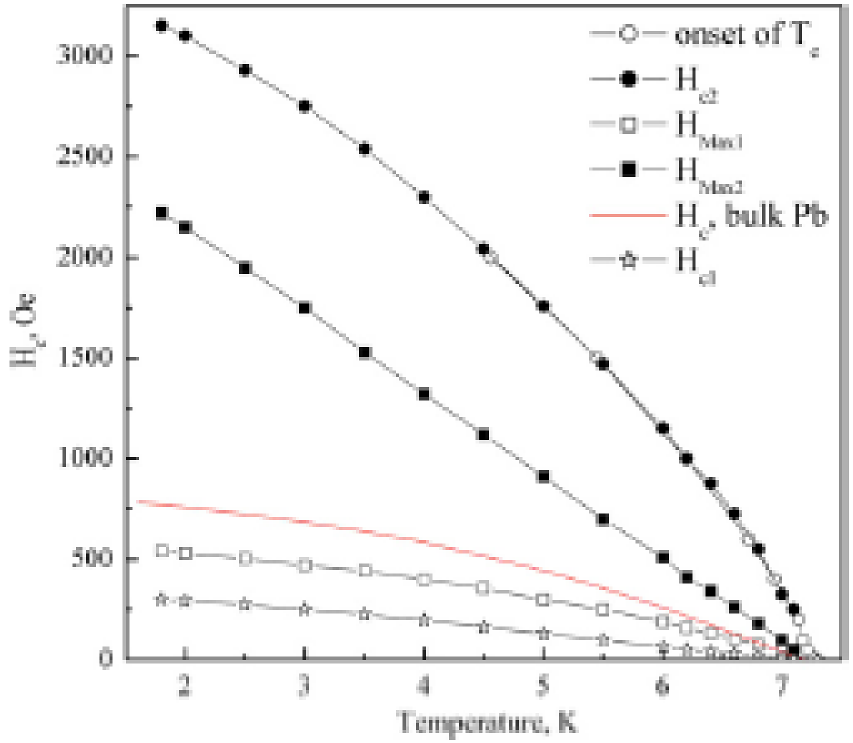

Fig. 6. Temperature dependence of various characteristic fields for lead inverse opal. The open circles are $T_c(H)$, the temperature of the onset of superconductivity. The solid circles correspond to the upper critical field H_{c2} at which a tangent to the rising branch of magnetization intersect the $H = 0$ line. $H_{Max\,1}$ and $H_{Max\,2}$ correspond to the two maximum on $M(H)$. H_{c1} is the lower critical field. The solid line is the $H_c(T)$ for the bulk Pb sample [32].

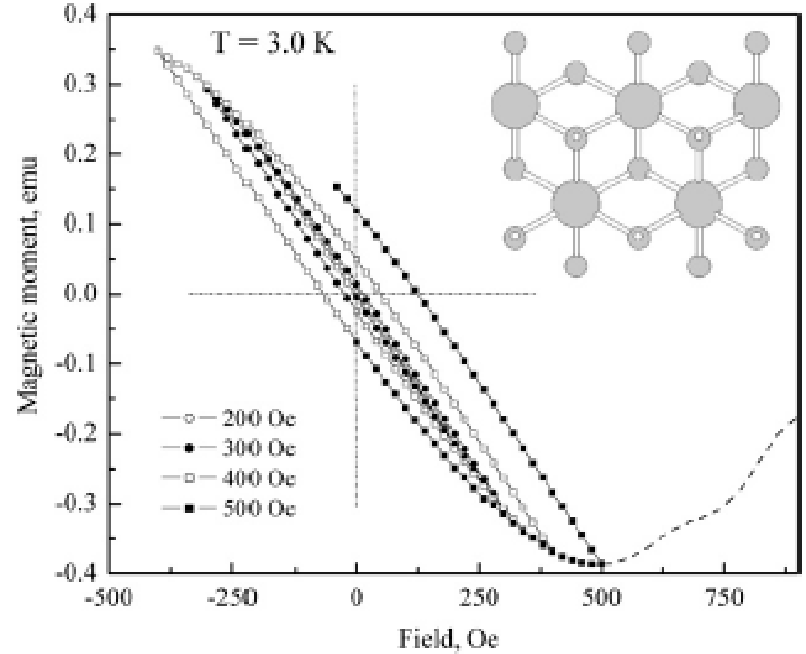

Fig. 5. Low-field hysteresis loop at the temperature 3 K. The loop closes at the lower critical field H_{c1}. Inset shows the fcc structure of opal pores infiltrated with Pb. Large spheres are octahedral pores ($r_{oct} = 62.1$ nm), and small spheres are tetrahedral pores ($r_{tetr} = 33.7$ nm).

Magnetoresistance in green Pb opal
T= 7.1 K, I = 0.5 mA, H along [111], I along [100]

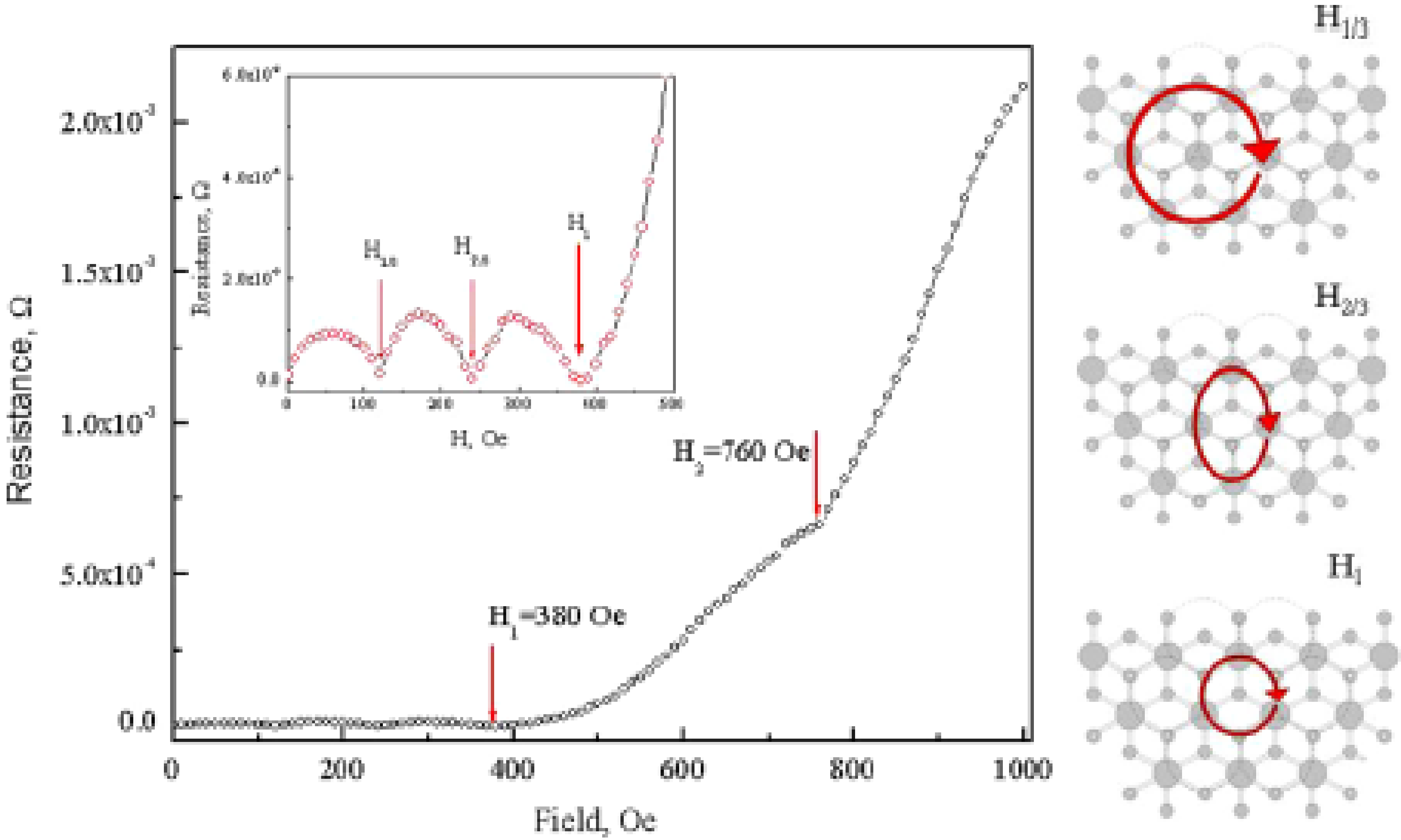

Appearance of new fluxoid phases in M with lowering T in blue Pb-Opal

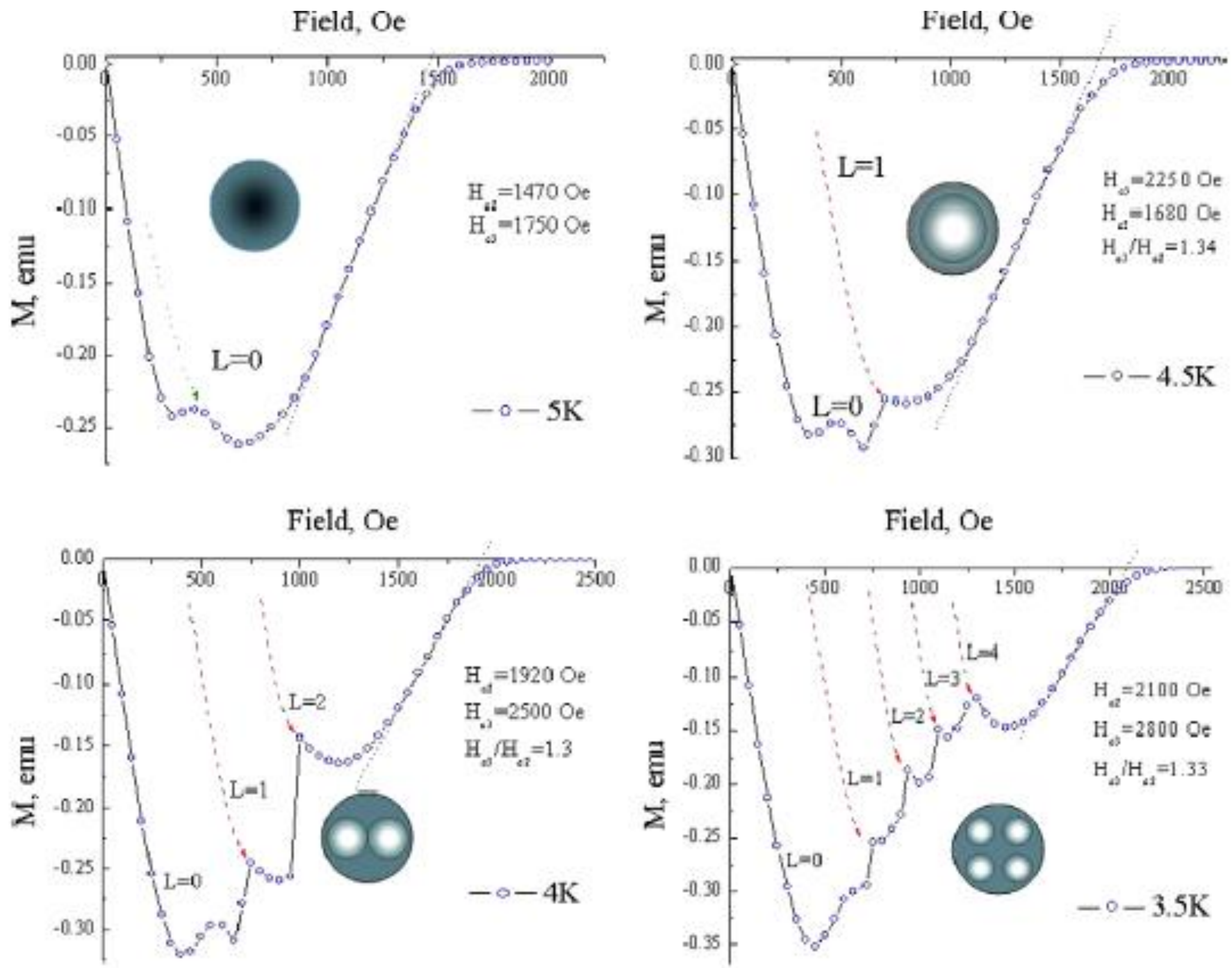

Low Field signal of MW absorption in Pb in Blue Opal

(160 nm spheres)

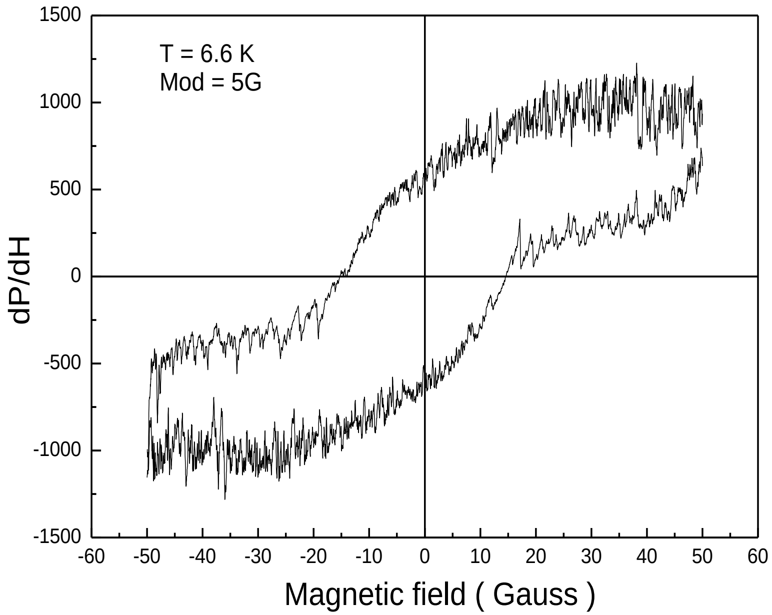

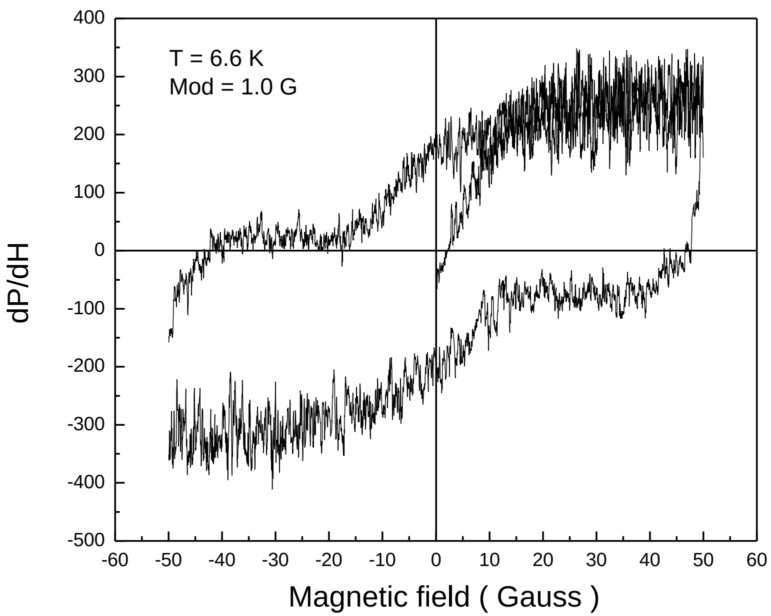

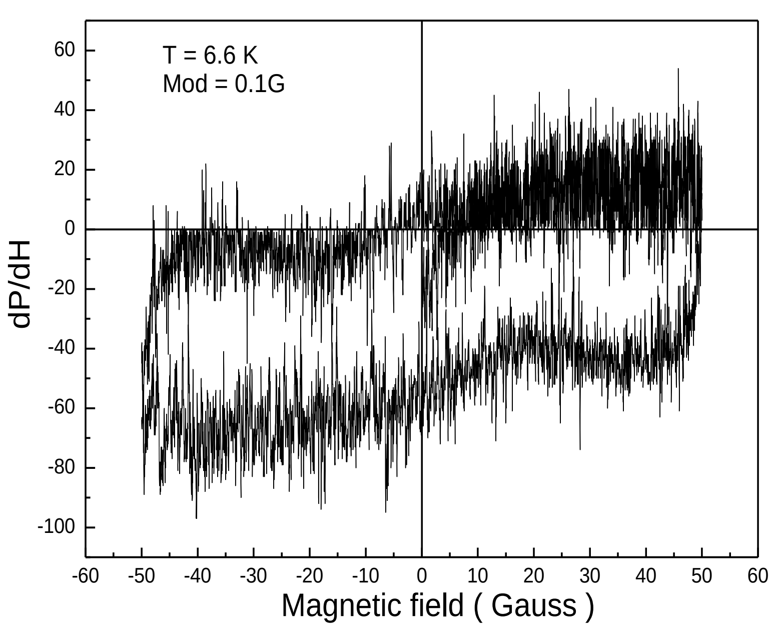

Low Field Signal of MW absorption on fluxons or weak link vortices always appear in SC below Tc

Microwave absorption studies of MgB_2 superconductor

M K BHIDE[1,*], R M KADAM[1], M D SASTRY[1], AJAY SINGH[2], SHASHWATI SEN[2], MANMEET KAUR[2], D K ASWAL[2], S K GUPTA[2] and V C SAHNI[2]

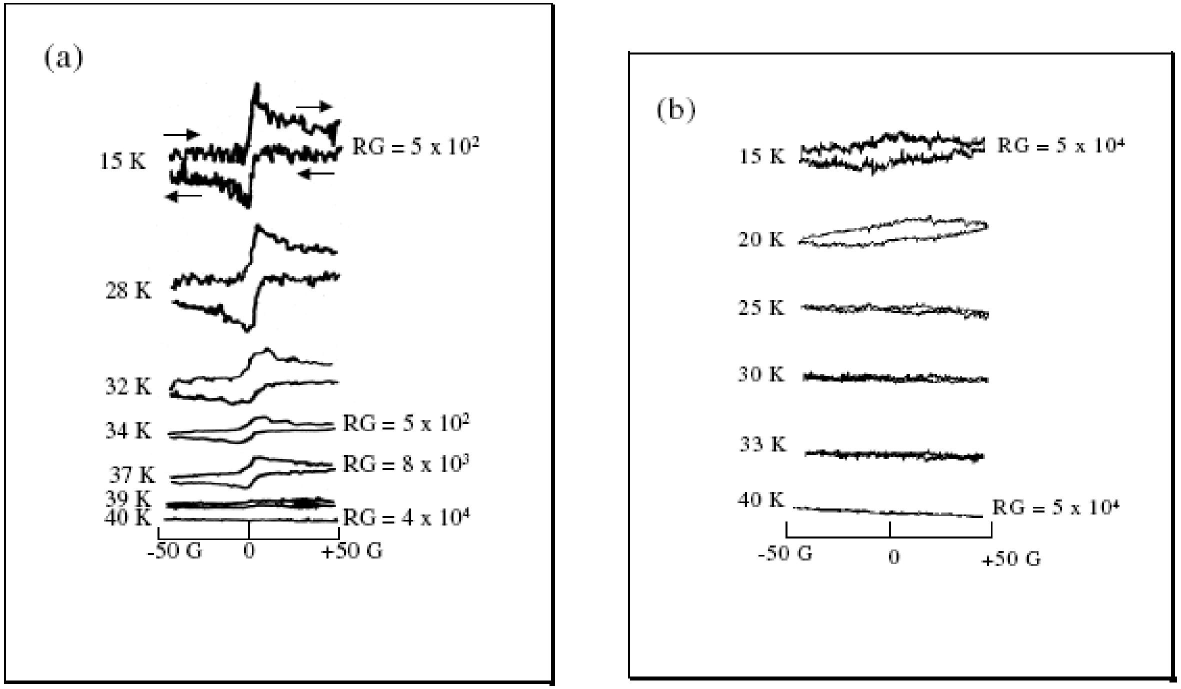

Figure 1. The temperature dependence of low field signal (LFS) recorded for (**a**) poly-crystalline and (**b**) single-grain MgB_2 samples.

LFS below Tc in Pb in red Opal

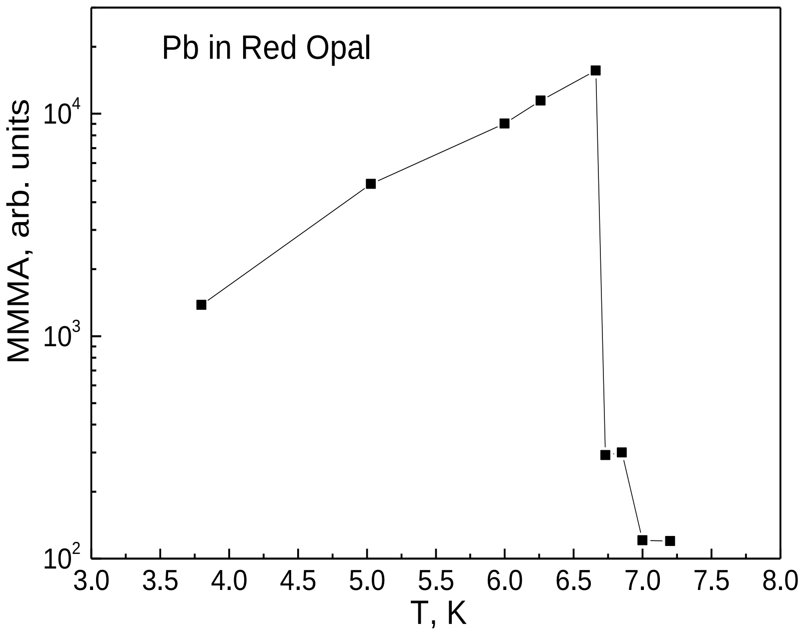

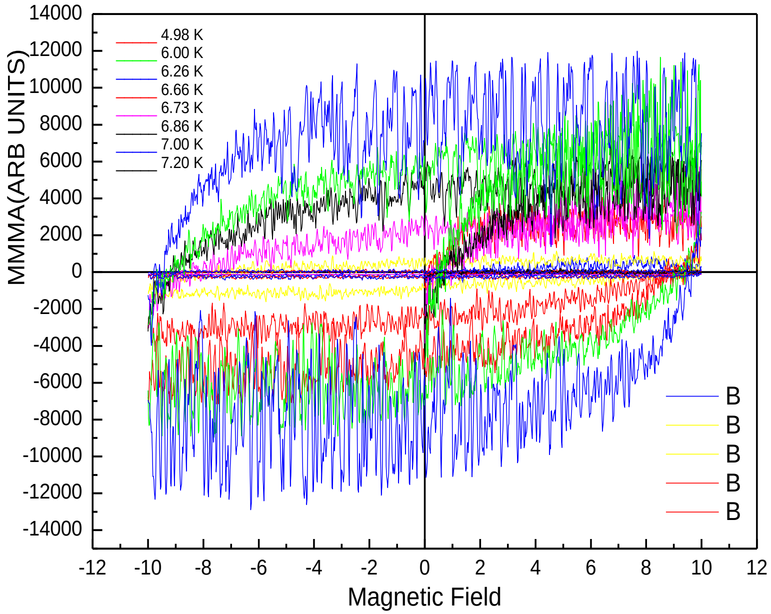

LFS below TC for Pb in Green Opal

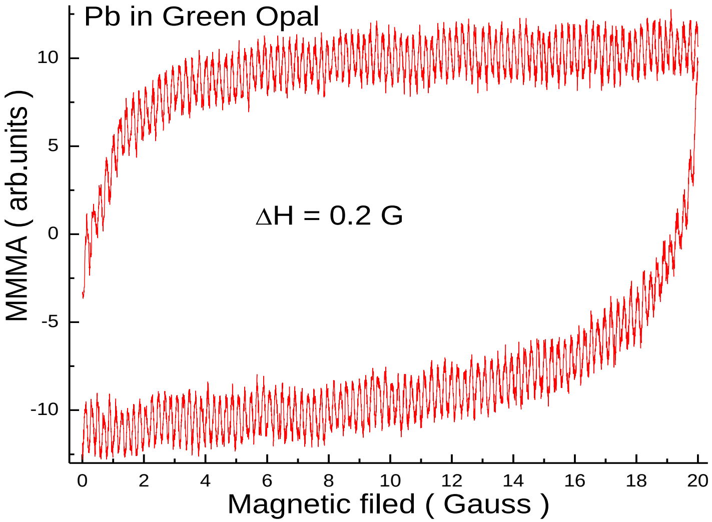

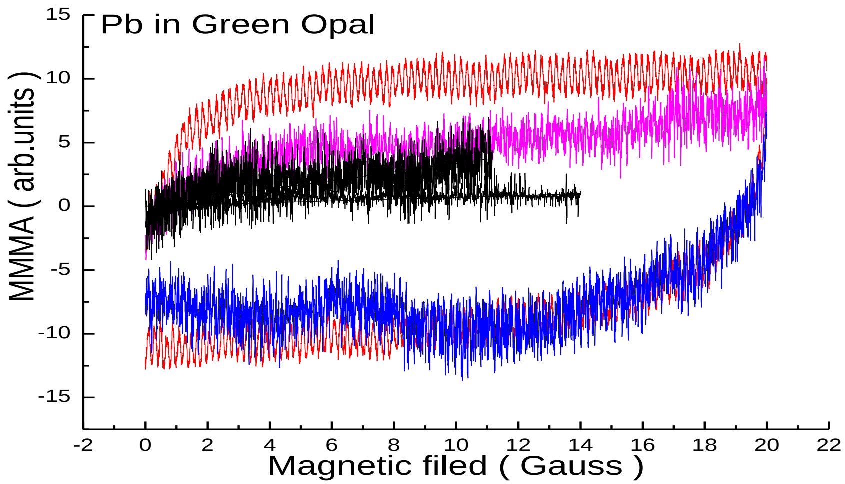

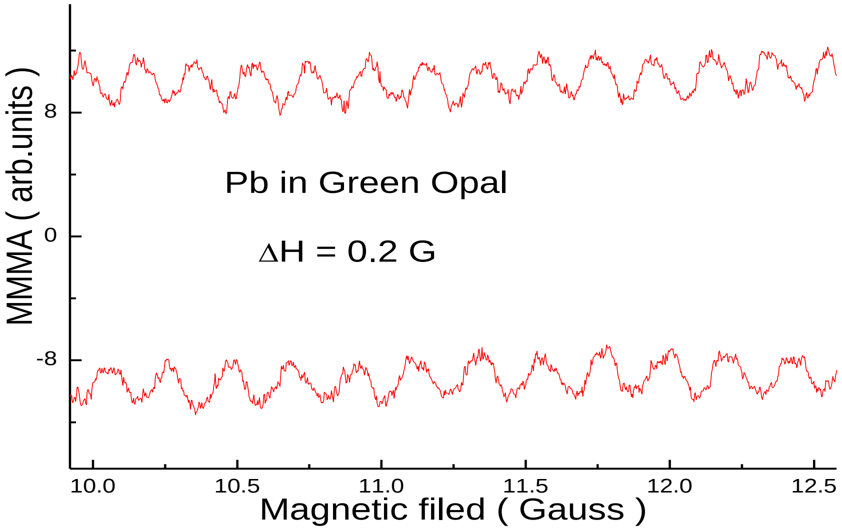

LFS in Pb in blue opal

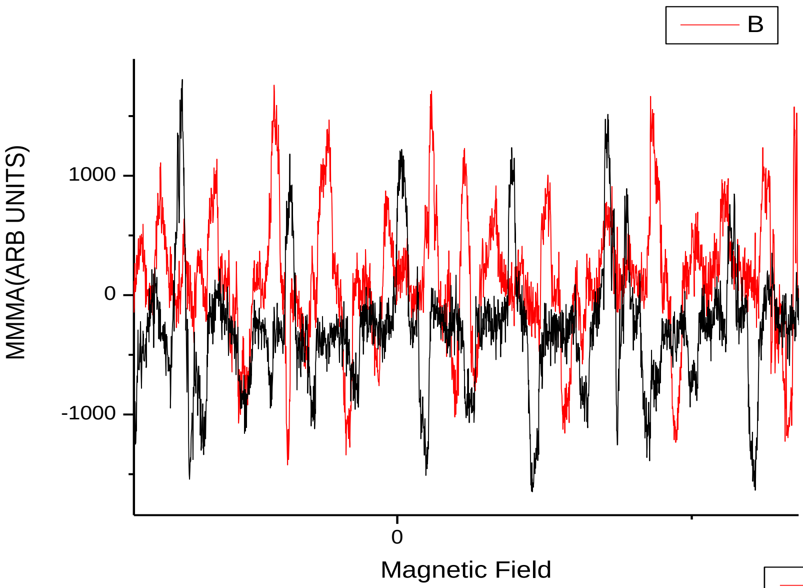

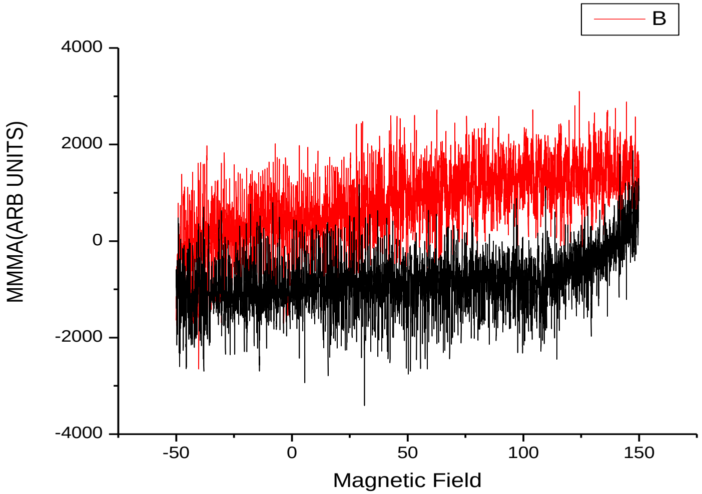

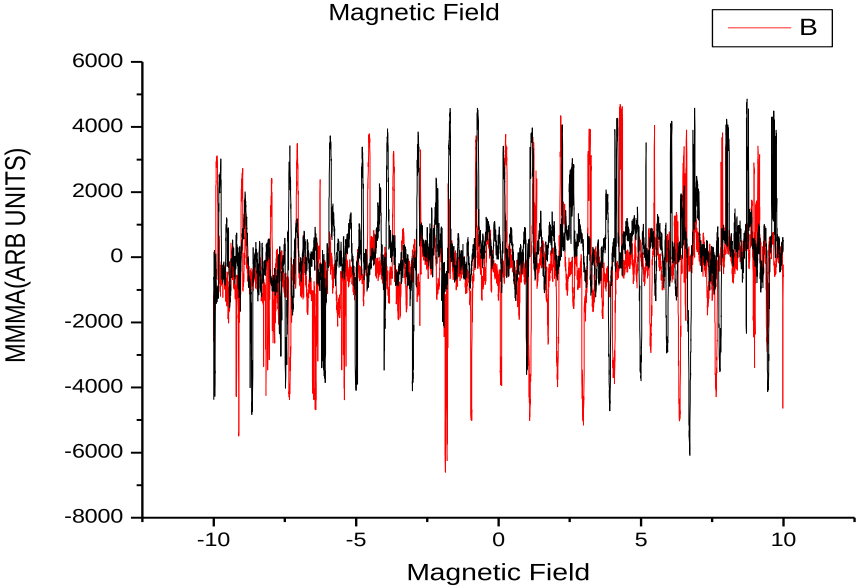

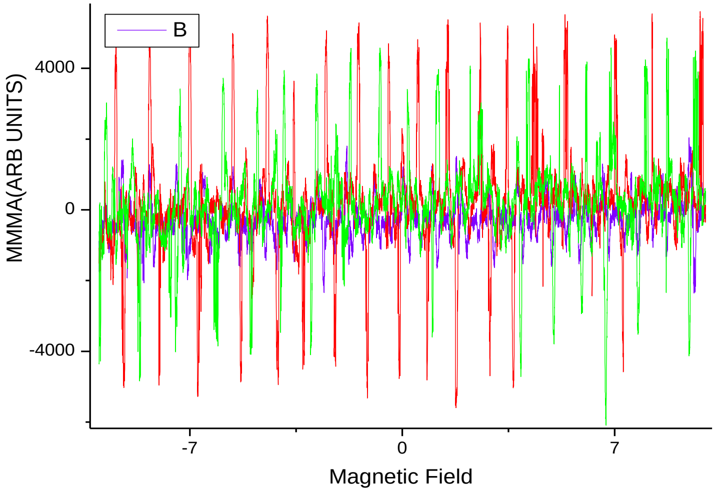

Comparison of discrete LFS in Pb-opals

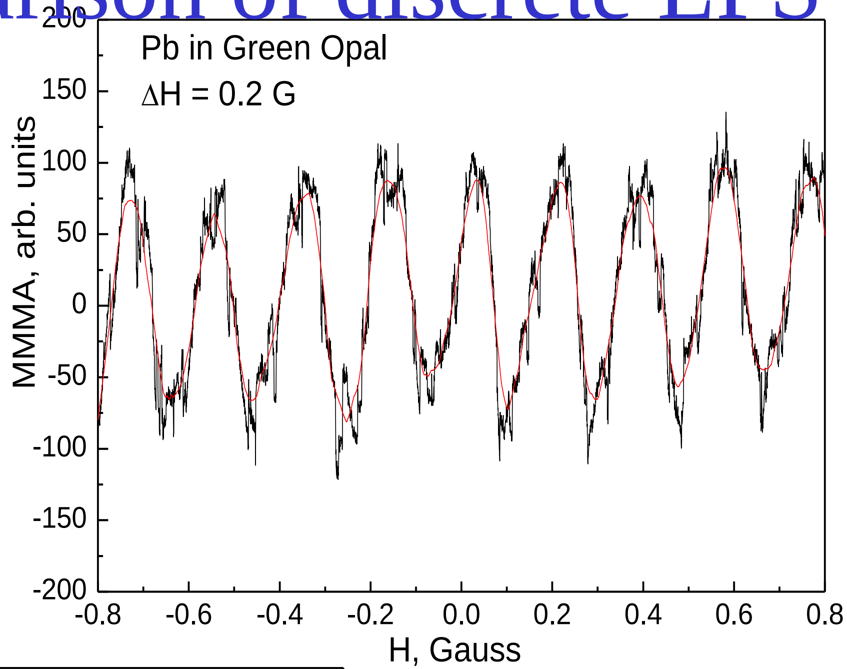

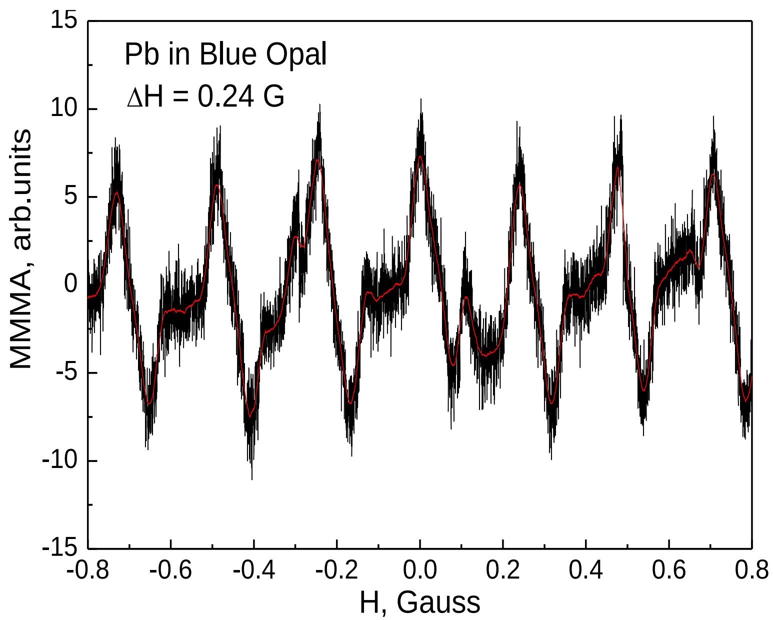

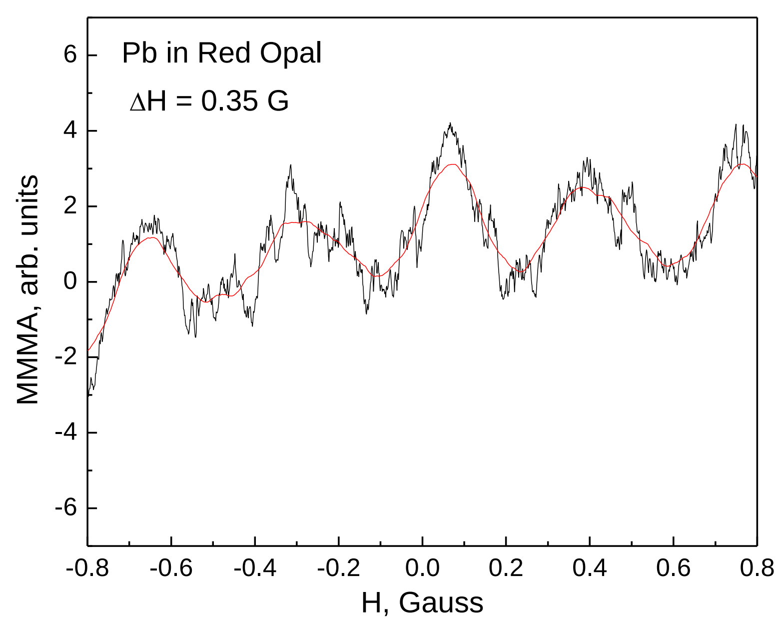

Low-field microwave absorption in single-crystal superconducting $YBa_2Cu_3O_{7-\delta}$

by K. W. Blazey
F. H. Holtzberg

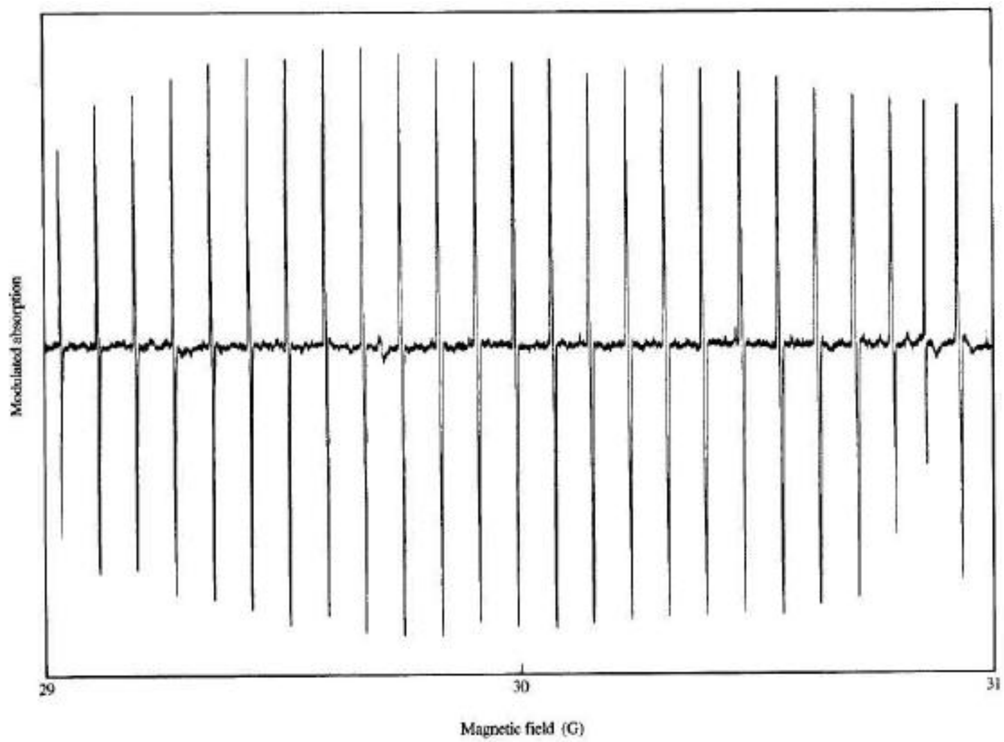

Figure 1

A segment of the 9.44 GHz microwave absorption line spectrum of a $YBa_2Cu_3O_{7-\delta}$ single crystal between 29 and 31 gauss at 4.3 K. The applied magnetic field is ⊥ ⟨c⟩ and ∥ ⟨110⟩, and the microwave field ∥ ⟨c⟩.

LFS in Pb FOIL: origin is the fluxons in grain boundaries

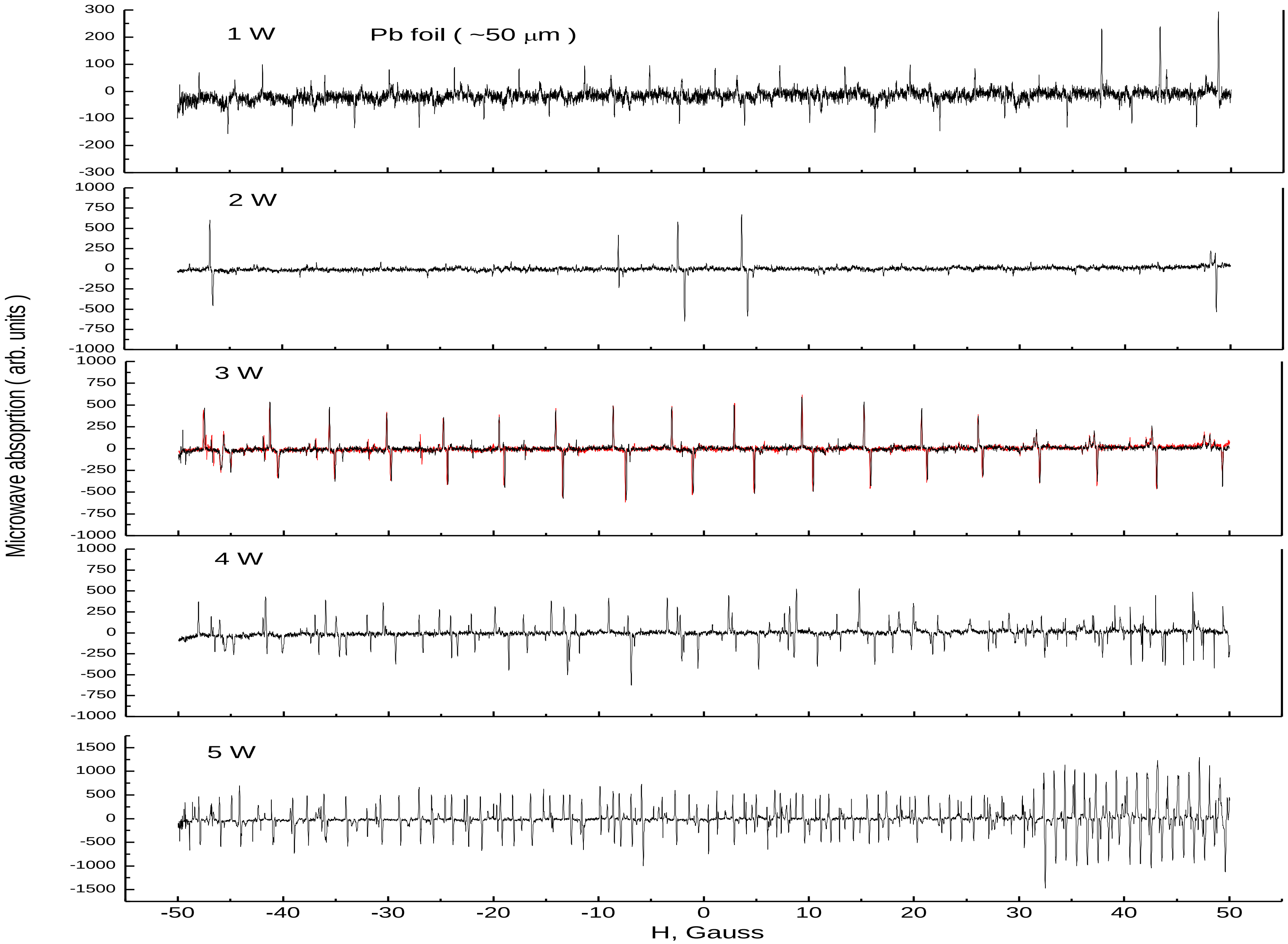

Conclusion to Part 1:
LTS in Nano-space

- Tc increase only slightly: from Tc=7. 1 to 7.32
- Critical field Hc2 increased 4-fold.
- Oscillations of M and R(M) demonstrate different fluxon phases.

- Huge interface of nanostructured SC can be used for tuning its properties

What next with Pb and other nano-LTS with extended interface?

- Try to self-assemble organic molecules with intensive Frenkel exciton transitions for extra “pairing glue” across the interface

- Can change Tc by changing concentration of carriers by “double layer charge injection”

Pb-Inverse Opal : Internal surface can be filled with "excitonic organic matter"

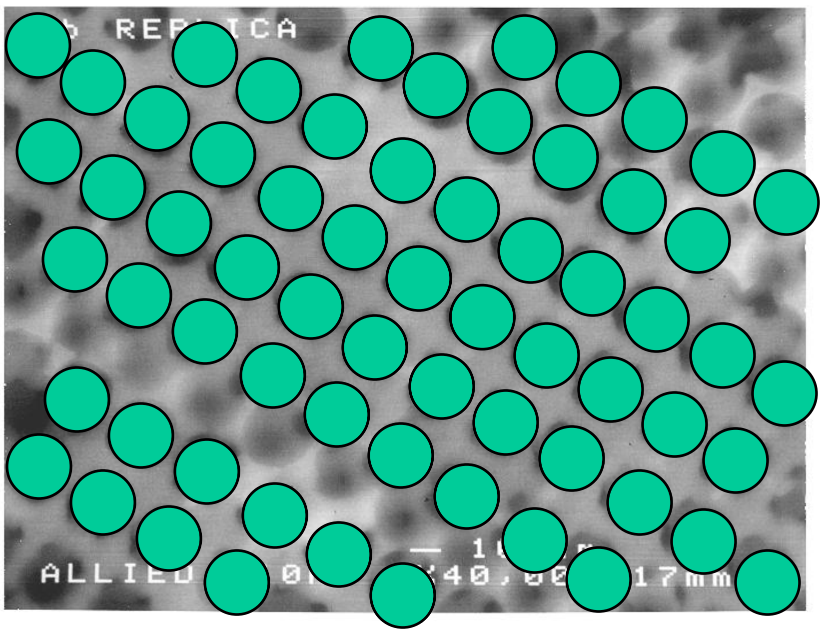

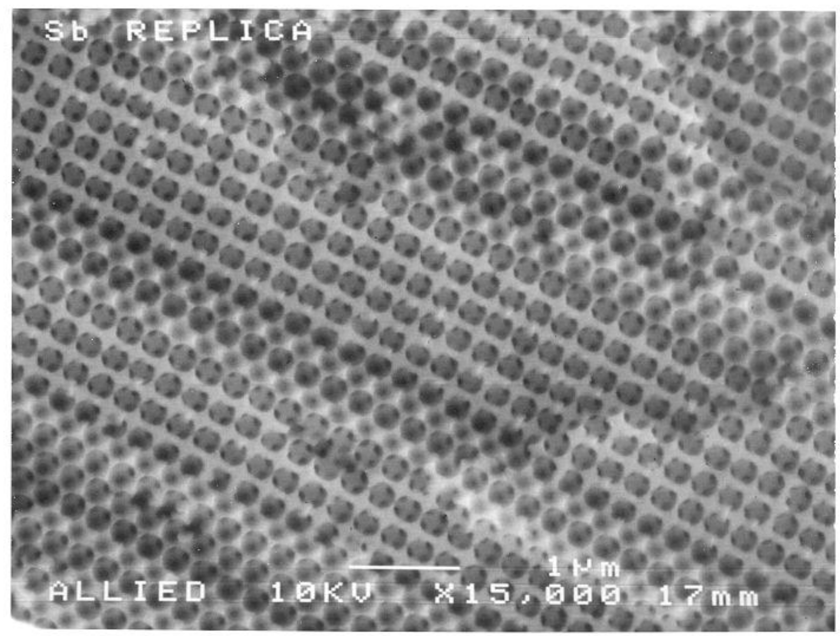

Part 2: Search for High Temperature Superconductivity in Na_xWO_{3-y} grown by Sol-Gel Route in Inverted Carbon opal

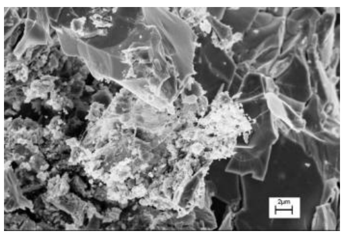

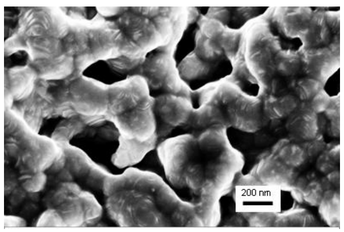

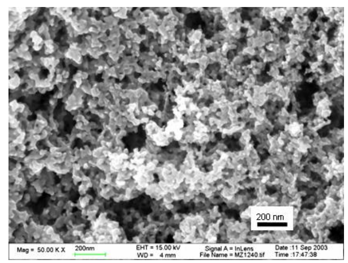

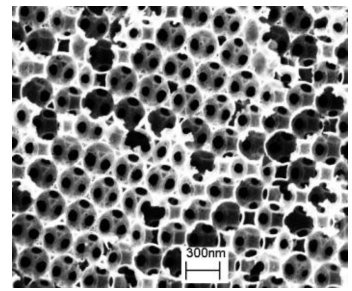

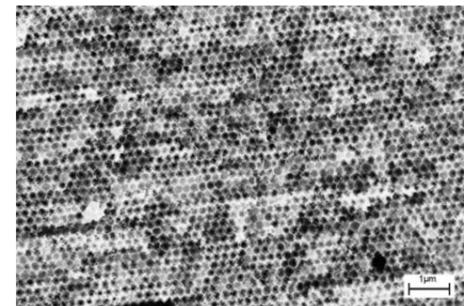

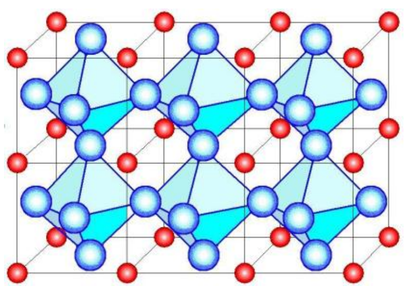

Motivation:

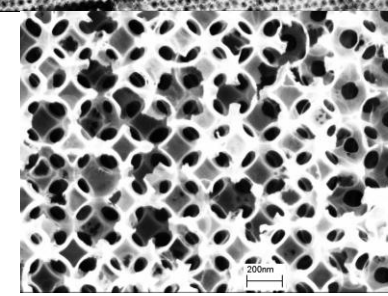

Confirm Diamagnetism around 91-100 K
Prove SC Tc by Low Field Signal of MW absorption
Try to understand the origin of High Tc

Outline for Part 2

- High Tc ~ 91-100 K in Na_xWO_3: is it USO

- Inverse carbon opals: matrices for sol-gel growth of WO_3

- Double layer electrochemical doping of Na
  by new “dry charging” method

- Magnetization results.

- Absence of LFMA: No SC ?

Eur. Phys. J. B 9, 1–4 (1999)

THE EUROPEAN PHYSICAL JOURNAL B

EDP Sciences

Rapid Note

Possible nucleation of a 2D superconducting phase on WO_3 single crystals surface doped with Na^+

S. Reich and Y. Tsabba

Department of Materials and Interfaces, The Weizmann Institute of Science, Rehovot 76100, Israel

Received 26 January 1999

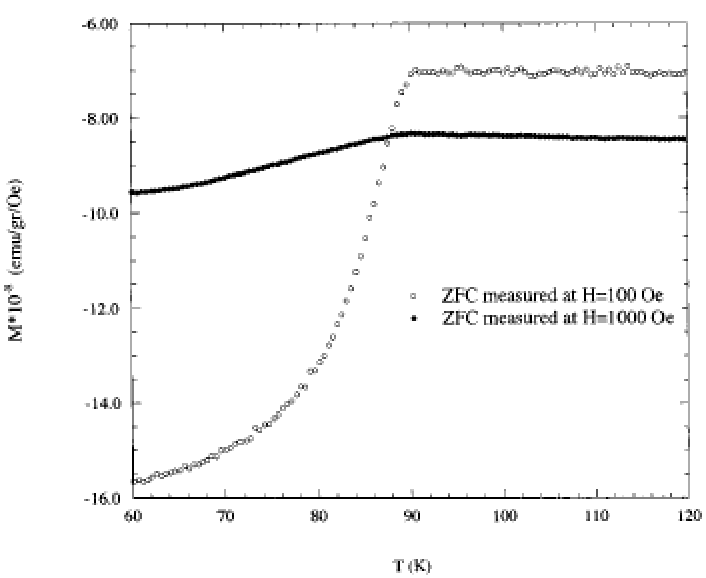

Fig. 3. Zero field cooled magnetic moment *vs.* temperature curves normalized by the magnetic field: (○) measured at 100 Oe; (●) measured at 1000 Oe in a heating cycle.

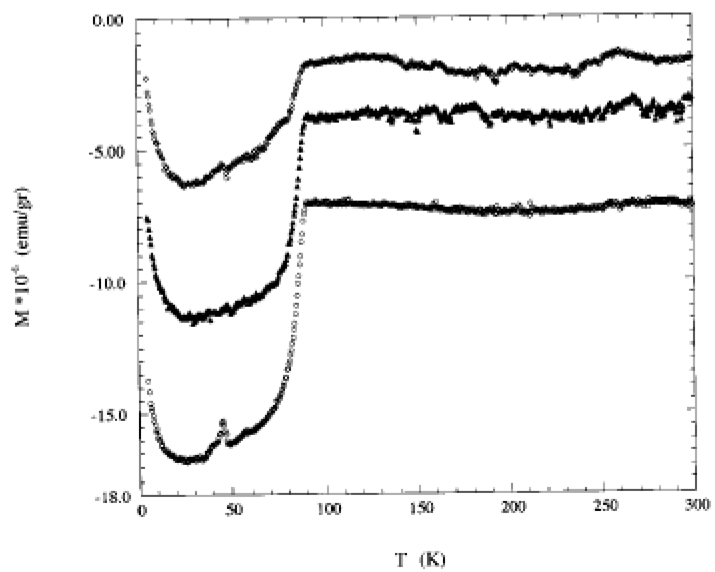

Fig. 7. Magnetic moment *vs.* temperature (ZFC) measured at 100 Oe in a heating cycle. (○) Bare crystals, (▲) crystals coated with gold after first sputtering process, (◇) after second sputtering process.

PHYSICAL REVIEW B, VOLUME 65, 144528

Concentration dependence of superconductivity and the order-disorder transition in the hexagonal rubidium tungsten bronze Rb_xWO_3: Interfacial and bulk properties

R. Brusetti,[1] P. Haen,[1] and J. Marcus[2]
[1]*Centre de Recherches sur les Très Basses Températures, associé à l'Université Joseph Fourier, CNRS, Boîte Postale 166, 38042 Grenoble Cedex 9, France*
[2]*Laboratoire d'Etudes des Propriétés Electroniques des Solides, CNRS, Boîte Postale 166, 38042 Grenoble Cedex 9, France*
(Received 10 October 2001; published 4 April 2002)

We revisited the problem of the stability of the superconducting state in Rb_xWO_3 and identified the main causes of the contradictory data previously published. We have shown that the ordering of the Rb vacancies in the nonstoichiometric compounds have a major detrimental effect on the superconducting temperature T_c. The

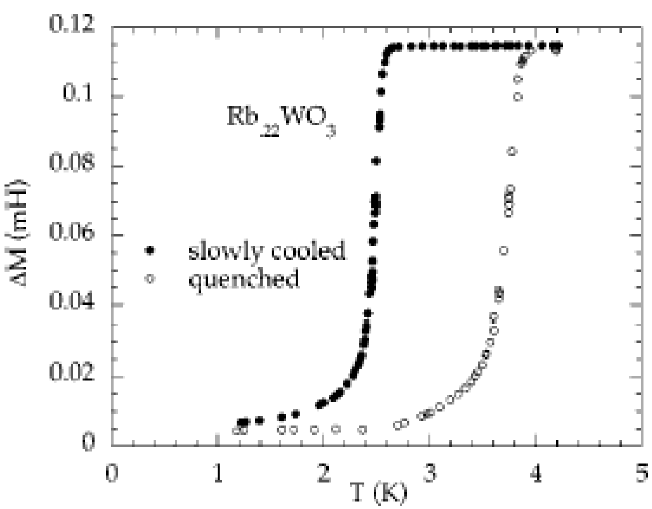

FIG. 1. Superconducting transitions (mutual-inductance variations) of a powder sample of $Rb_{0.22}WO_3$ after different cooling rates.

B. Calorimetric study of the order-disorder transformation

After several unsuccessful attempts, we finally observed the enthalpy anomaly accompanying this transformation, but

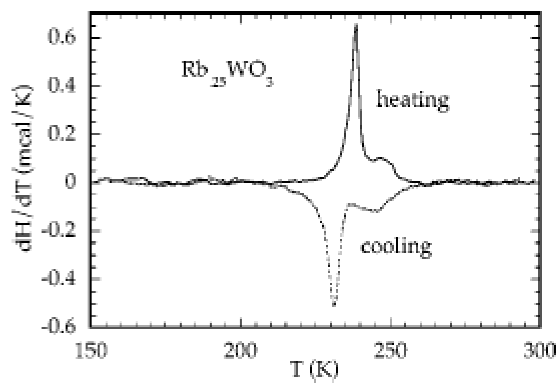

FIG. 2. DSC thermograms observed on a powder sample of $Rb_{0.25}WO_3$ (≈ 50 mg) on heating and on cooling at ± 10 K/min.

Tc dependence on x: disorder driven SC in RbxWO3

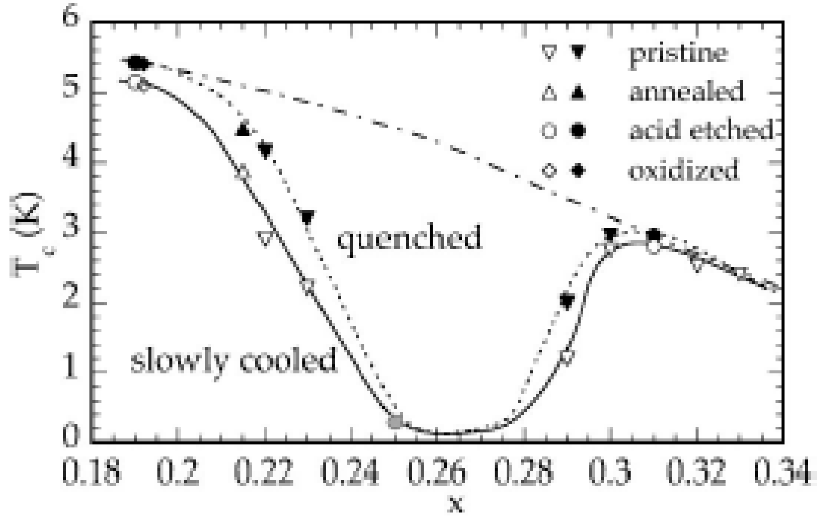

FIG. 9. The superconducting transition T_c as a function of the rubidium content x. Empty or full markers refer to measurements after slow cooling or quenching from ≈ 300 K, respectively. The grey marker corresponds to an intermediary cooling in a ^3He-^4He dilution refrigerator. The curves are only guides to the eye and the monotonous one extrapolates what we think would be the $T_c(x)$ dependence if the vacancy ordering could be prevented.

Interfacial SC with high Tc

superconductivity also develops on the surface of WO_3 crystals that have been subjected to a slight superficial enrichment of sodium.[5] The very high T_c's observed in the latter case (up to 91 K) is evidently far from being explained but indicates how much the interfacial properties of these materials could be promising. The great versatility of the WO_6 octahedra we discussed above, certainly plays a part in these superficial or interfacial properties.

Carbon Inverted Opal: Intensely Colorful and Highly Conductive

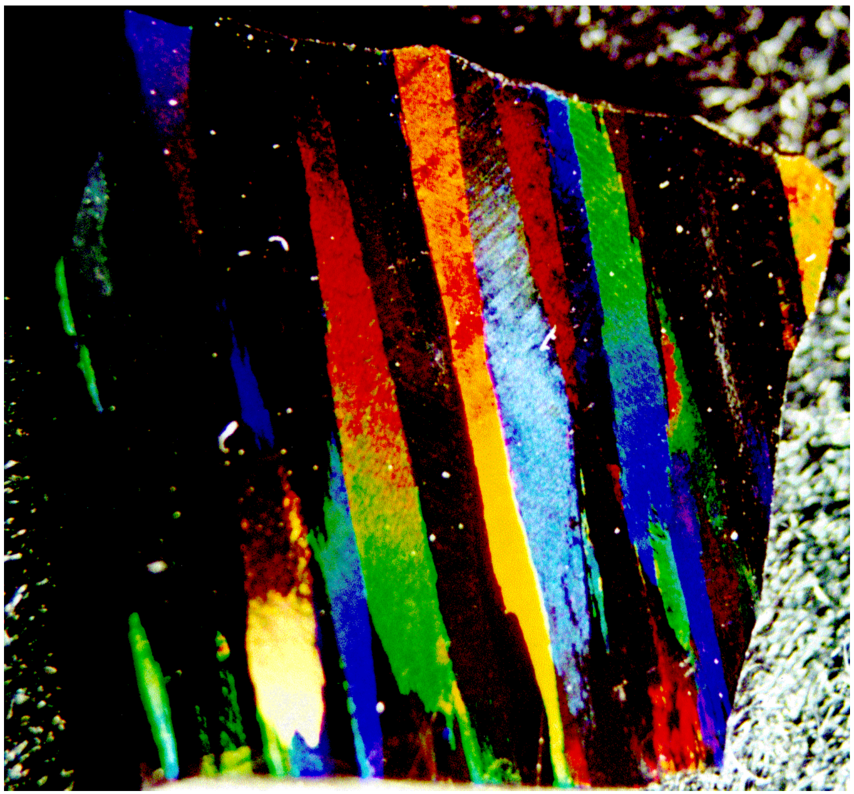

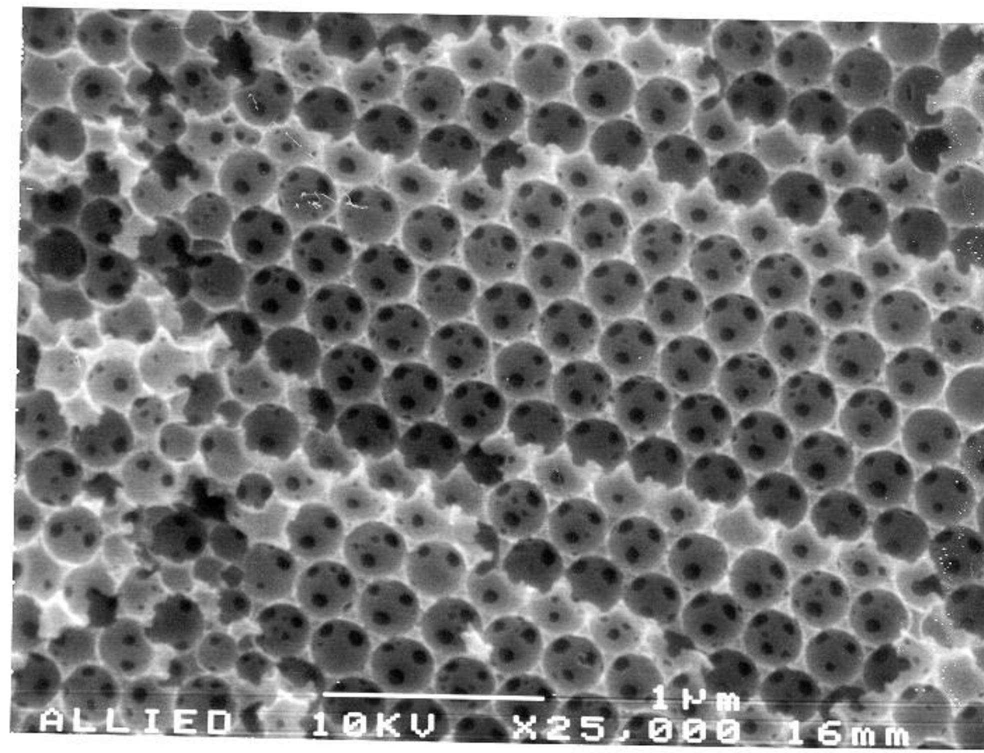

What we need to make a good Na_xWO_3

1. Huge Interface

2. Synthesize WO3 at interface
   of nanocarbon

1. Coat it with:
   - with Na ions layer
     by electrochemistry

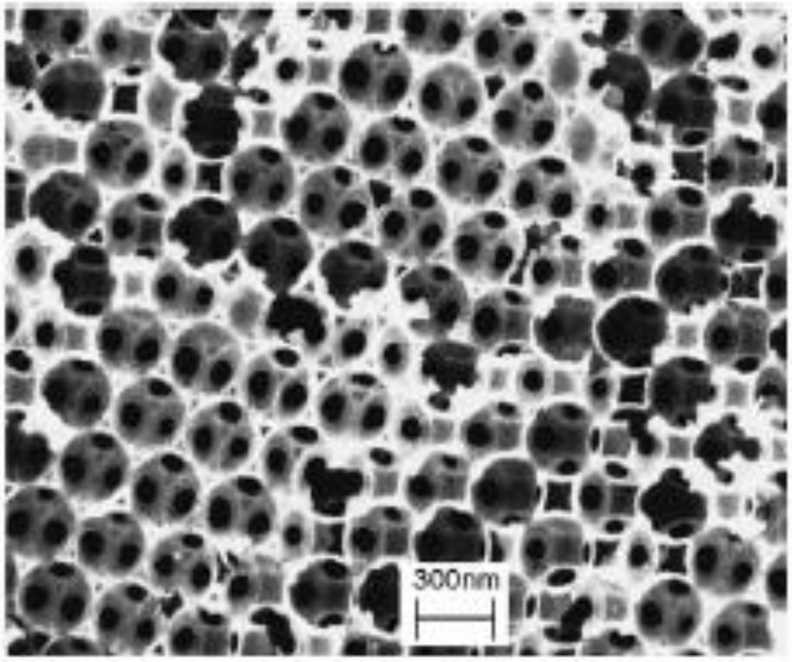

NaxWO3 in Inverted Carbon Opals:

1. Porous matrix for WO_3 growth by sol gel
2. WO_3 coated nano-carbon: good electrode for electrochemical Na doping

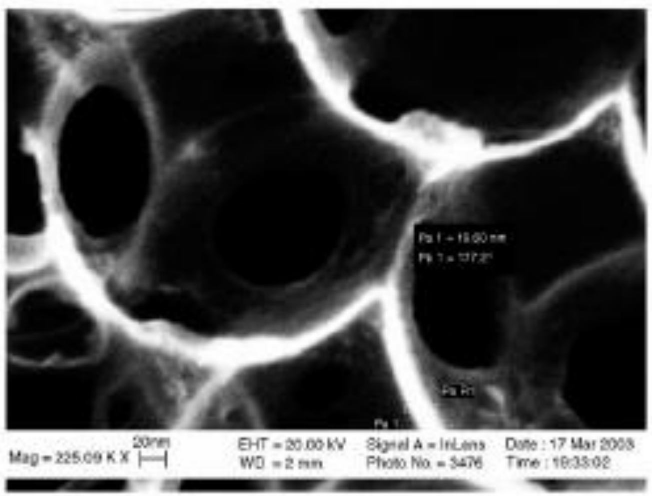

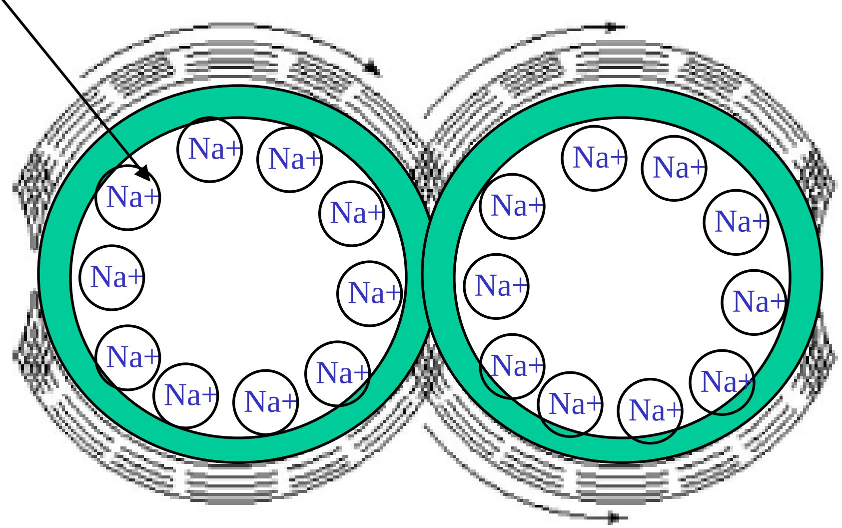

Search for Superconducting Materials Using Frozen Giant Interfacial Charge Injection

BACKGROUND: Charge injection could enable performance optimization for superconducting materials enhancing Tc.

However, dielectric charge injection in FETs is normally not in the bulk and is normally small and short-lived.

GOAL: *Tune Superconducting* material properties using giant frozen charge transfer at huge interfaces in WO3-inv. opal

Examples: NaxWO3 created by sol-gel in conductive carbon inverse opals, doped by Na, via charge injection in NaCl: observation of diamagnetic transition at 125 K, but no LFMA (?)

Properties Changes Possible From Frozen Interfacial Charge Transfer

Optimize (or generate)

- Superconductivity
- Ferromagnetism
- Electrical conductivity
- Optical properties
- Thermal conductivity
- Catalytic activity
- Absorption (sensing)
- Thermoelectric ZT

Transition between anti-ferromagnetic and superconducting behavior as a function of charge concentration for high T_c superconductors.

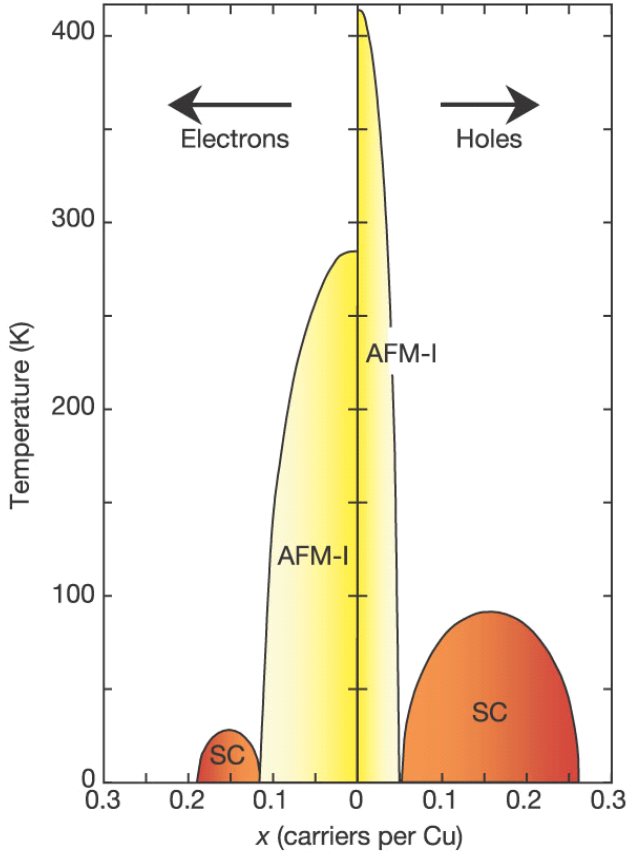

Methods of Charge Injection

Polyacetylene

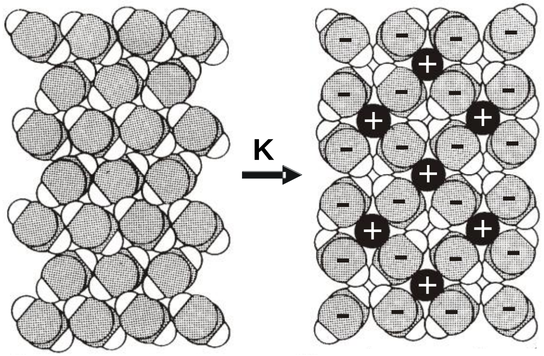

- DOPANT INTERCATION CHARGING: Fundamentally *changes structure*, *adds defects*, requires *slow bulk diffusion*, and is *not fully reversible*.

- ELECTROSTATIC CHARGING: *Stores little charge or requires high voltages and requires electrode proximity.*

C= charge/voltage

C= area × dielectric constant /d

- INTERFACIAL DOUBLE-LAYER CHARGING: *Stores high charge at low voltage, but needs electrolyte.* ***SURPRISES WILL BE SHOWN!***

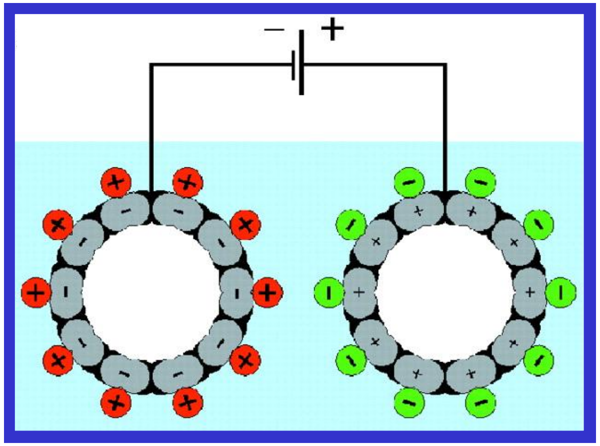

d is in nms

Our Strategies for Obtaining Frozen Interfacial Charge Transfer

All strategies use conducting materials having very large surface areas (above 100 m^2 gm^{-1}/density)

Electrochemical double-layer charge injection followed by removal from electrolyte.

WE SHOW THAT ELECTRODES WITH GIANT CHARGE INJECTION ARE SEPARATABLE WITHOUT LOSING CHARGE!

TRICK: COUNTERIONS PREVENT COULOMB EXPLOSION.

Prototype High-Surface-Area Material

(We are now doing the same experiments for compacted Pt nanoparticle electrodes)

- Charge SWNT electrodes in 1M NaCl – show CV of classical interfacial double-layer charge injection.

- Demonstrate about 10 fold conductivity increase from hole injection.

- Remove charged-injected electrode from electrolyte – show increased conductivity is maintained even after exposure to dynamic vacuum for 3 hours.

- Re-immerse electrode in electrolyte and show by electrochemical measurements that the charge is maintained.

Cyclic Voltametry Indicates Classical Behavior for Double-Layer Charging

(Annealed HiPco SWNTs in 1 M NaCl)

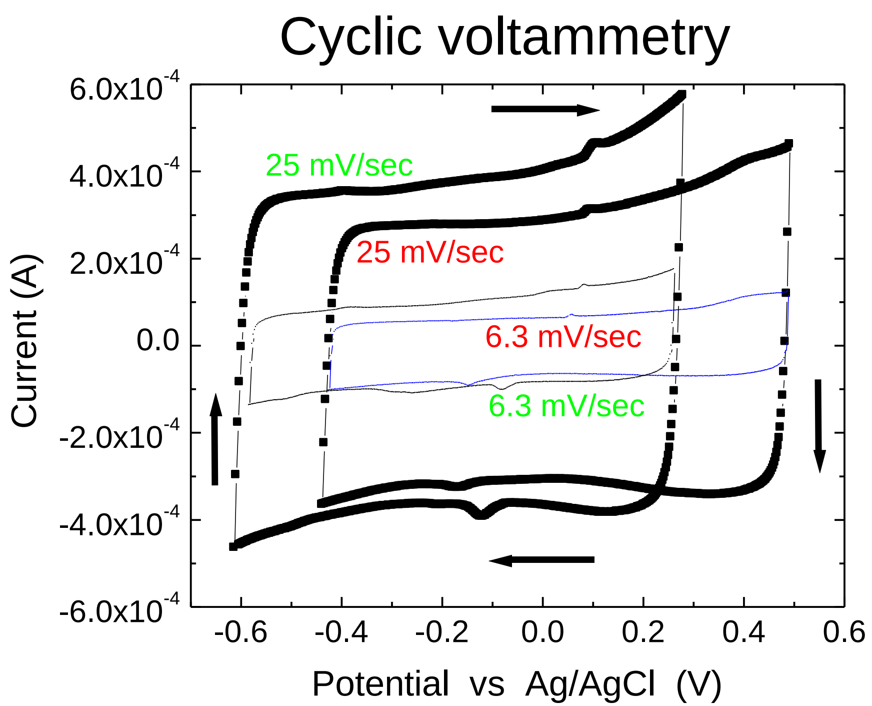

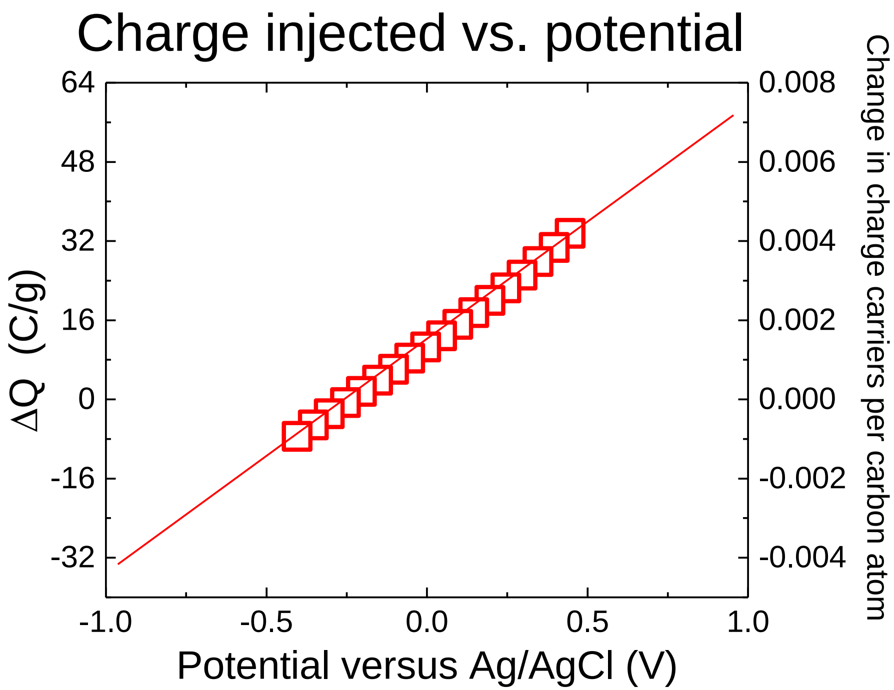

Capacitance of 22 F/g increases slightly (to 28 F/g) with increasing cycling – likely due increased SWNT wetting.

Injected charge can be increase by increasing the redox stability window of the electrolyte (<2 V TO 5 V).

Minor Faradic peaks are a problem, and can be eliminated.

Four-Probe Electrical Conductivity Increases About Order of Magnitude Upon Hole Injection

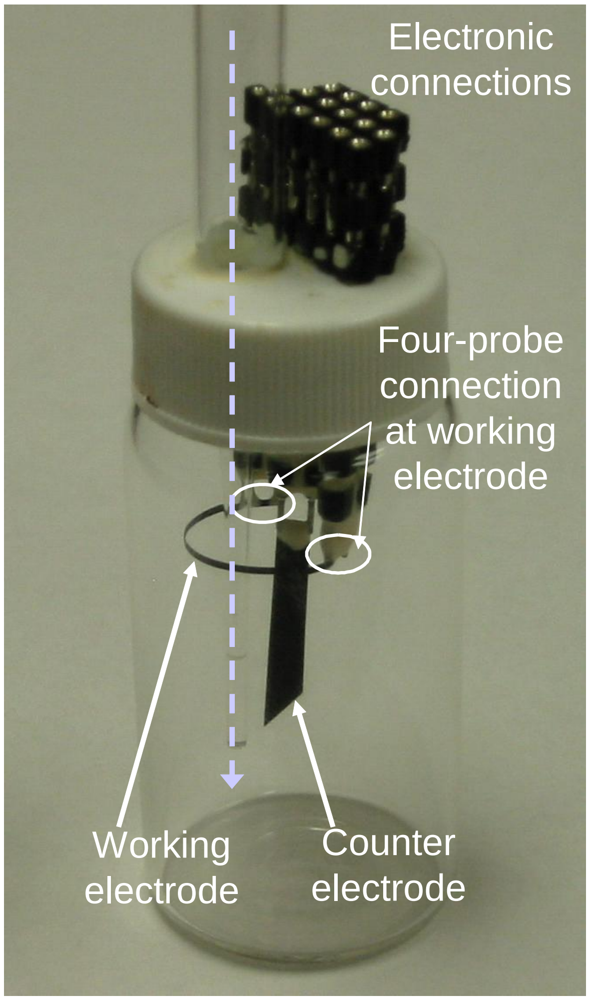

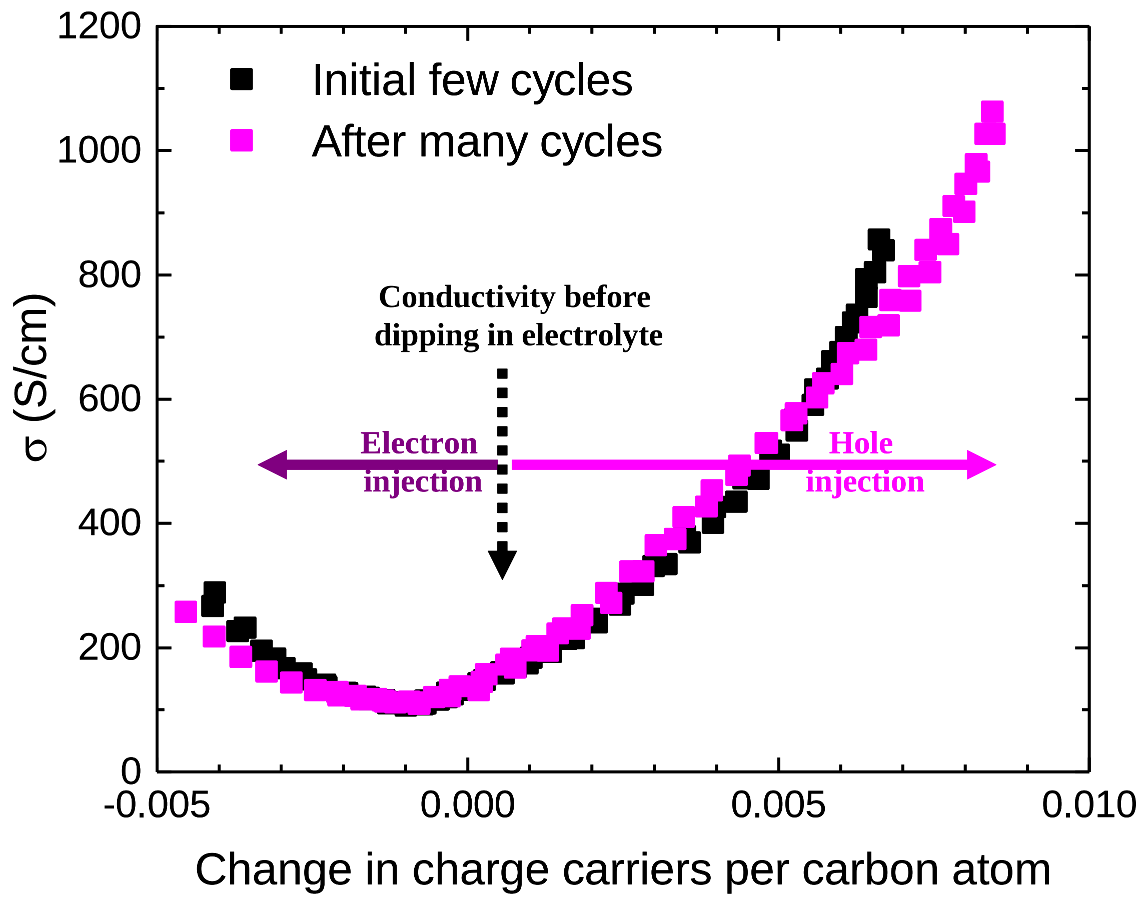

Ion-containing Interface Water
Solvated (right) or Unsolvated (left)?

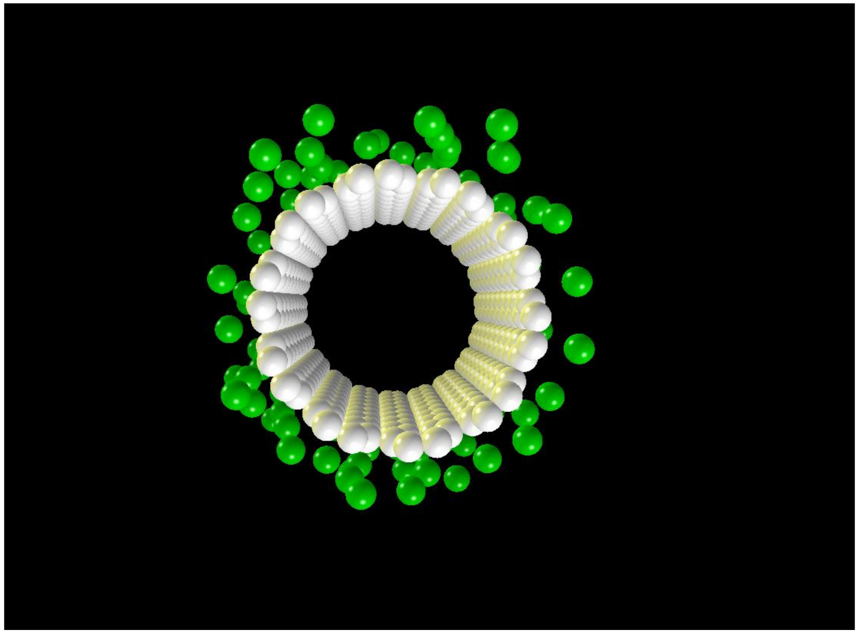

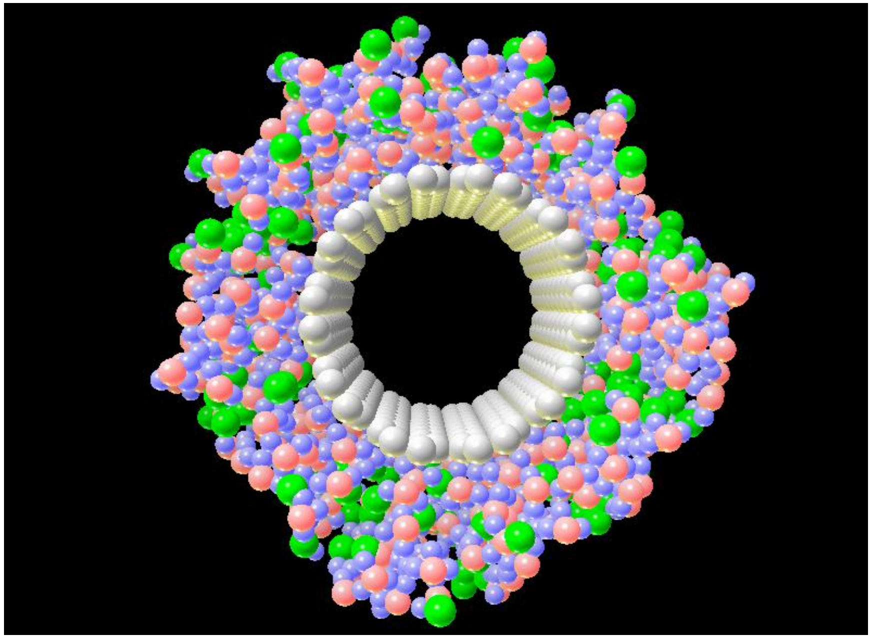

Atom designations: Cl^- (green) carbon (white), hydrogen (blue), oxygen (red).

These Processes Work for Any Nanoscale Conductor

Example: Metal nanoparticles molded into shaped articles, molten electrolyte is injected, charge is electrochemically injected, then electrolyte is "frozen".

Evidence[1,2] that metals will work just like nanotubes:

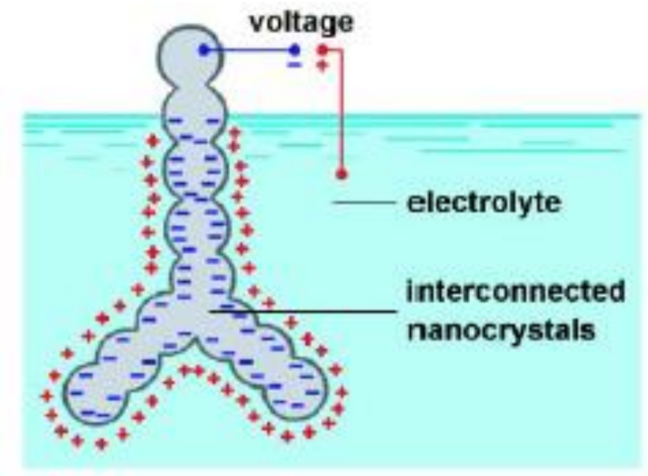

Weissmuller *et. al. Science* **300,** 312 (2003)
Baughman, *Science* **300,** 268 (2003)

Double-layer charge injection increases unit cell volume of Pt by ~0.4%.

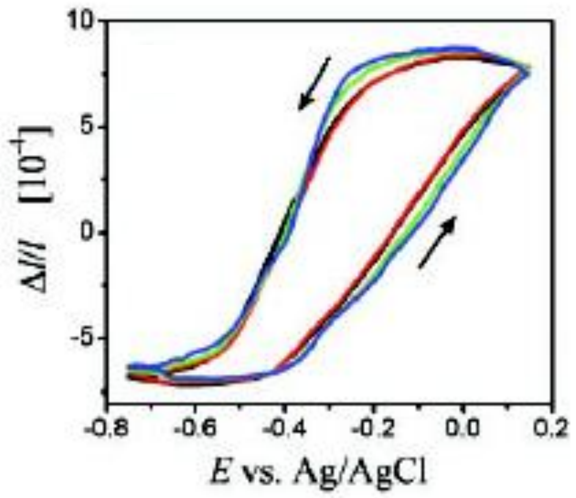

Preparation of Na_xWO_3 Inverted Opal

- We used a sol-gel technology for preparation WO3 film in porous nanostructured host matrices.
- Sol-gel technology allows to vary the structural parameters and concentration of composition in wide range.
- To increase the volume fraction of superconducting phase we infiltrated WO3 into nanoporous material with high surface area and then electrochemically doped to obtain double layer with alkali ions (Li+, Na+, K+).

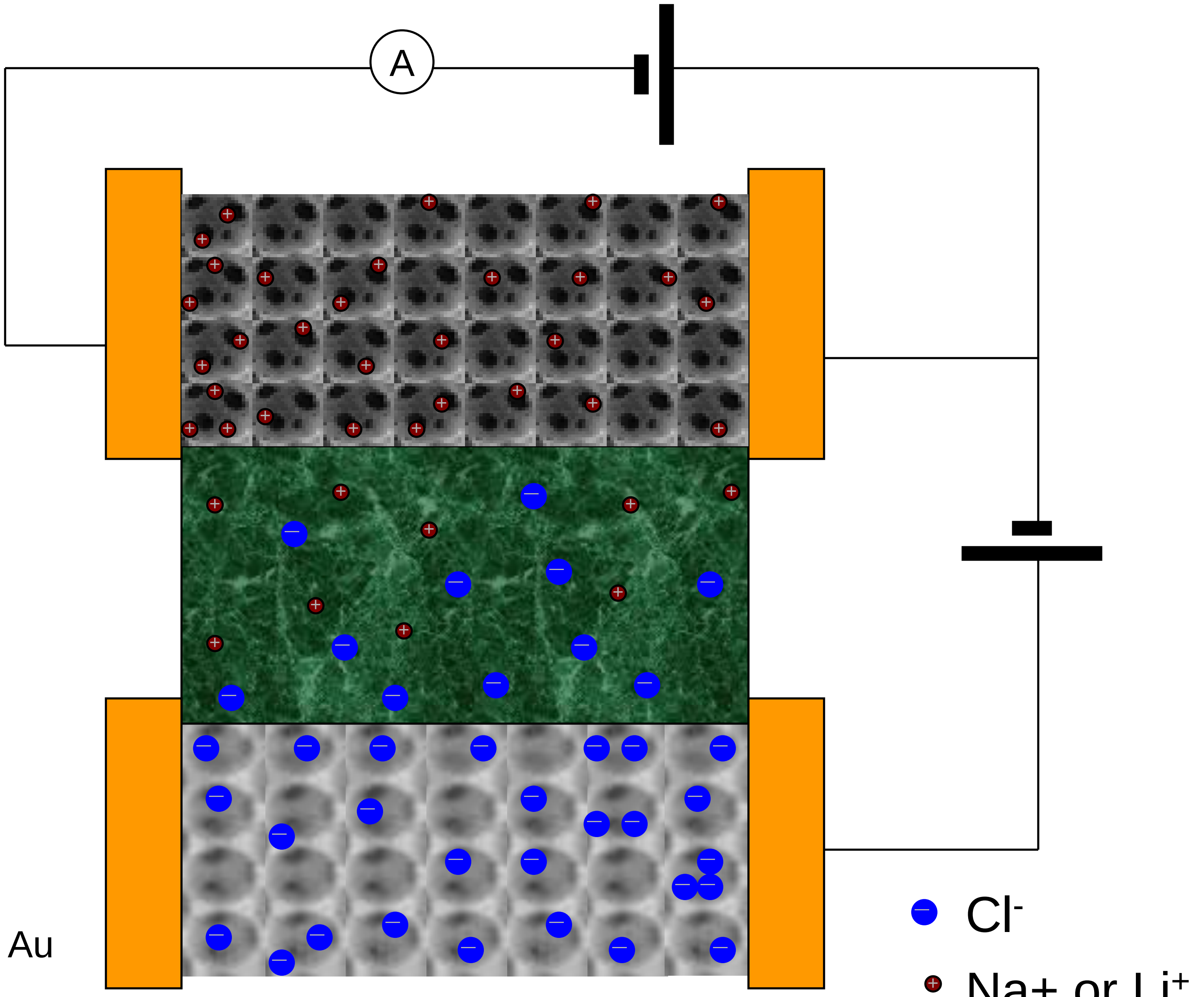
A
Au
Cl-
Na+ or Li+

ZFC magnetization: Diamagnetic drop at T=125-130 K

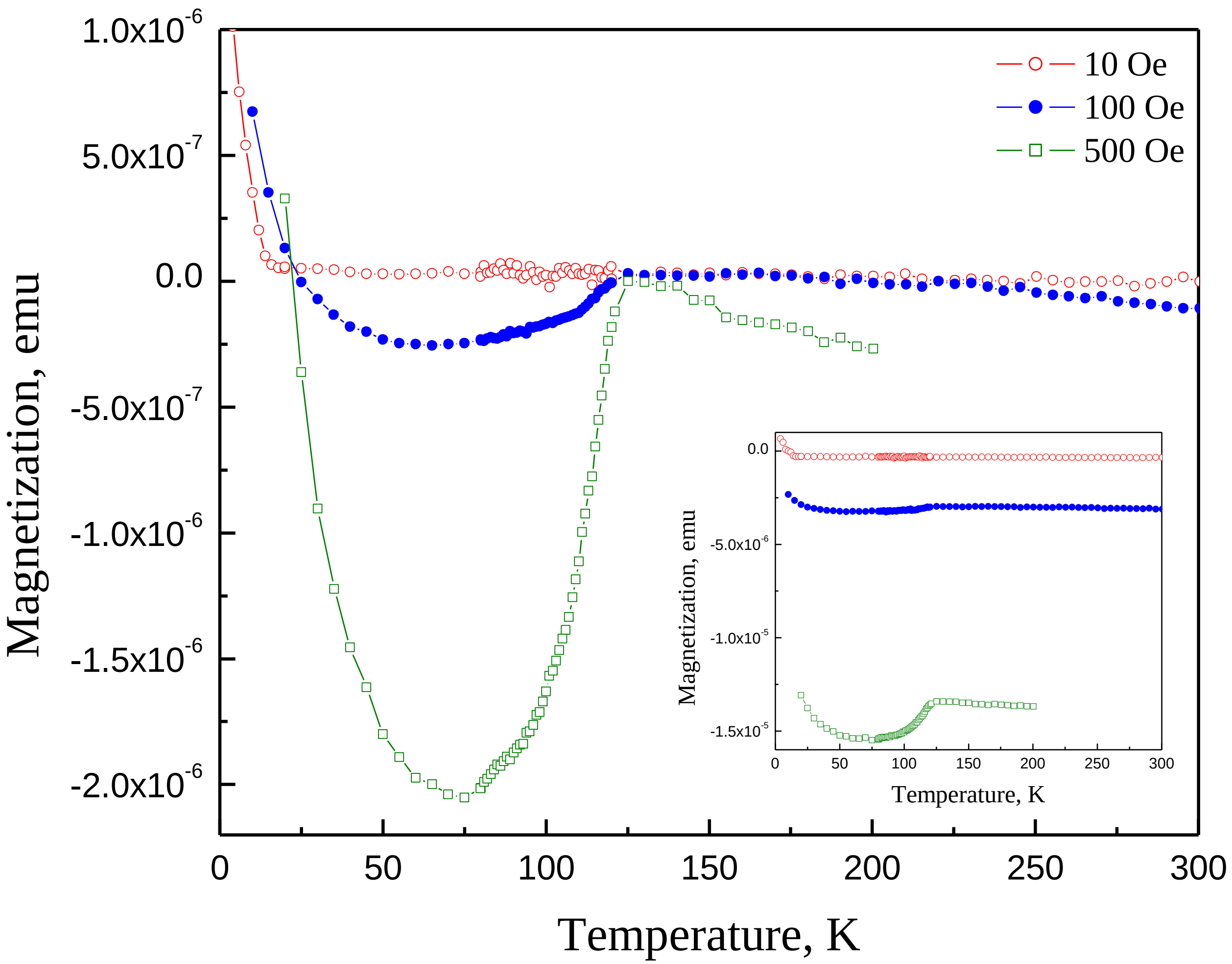

The temperature dependence of ZFC magnetization for Na_xWO_{3-y} infiltrated into carbon inverted opal at three different applied fields: 10, 100 and 500 Oe. For comparison all three curves were bound to M=0 at T=130 K by subtraction the contribution from host matrix. Inset shows the real distribution of measured magnetization.

FC and ZFC magnetization

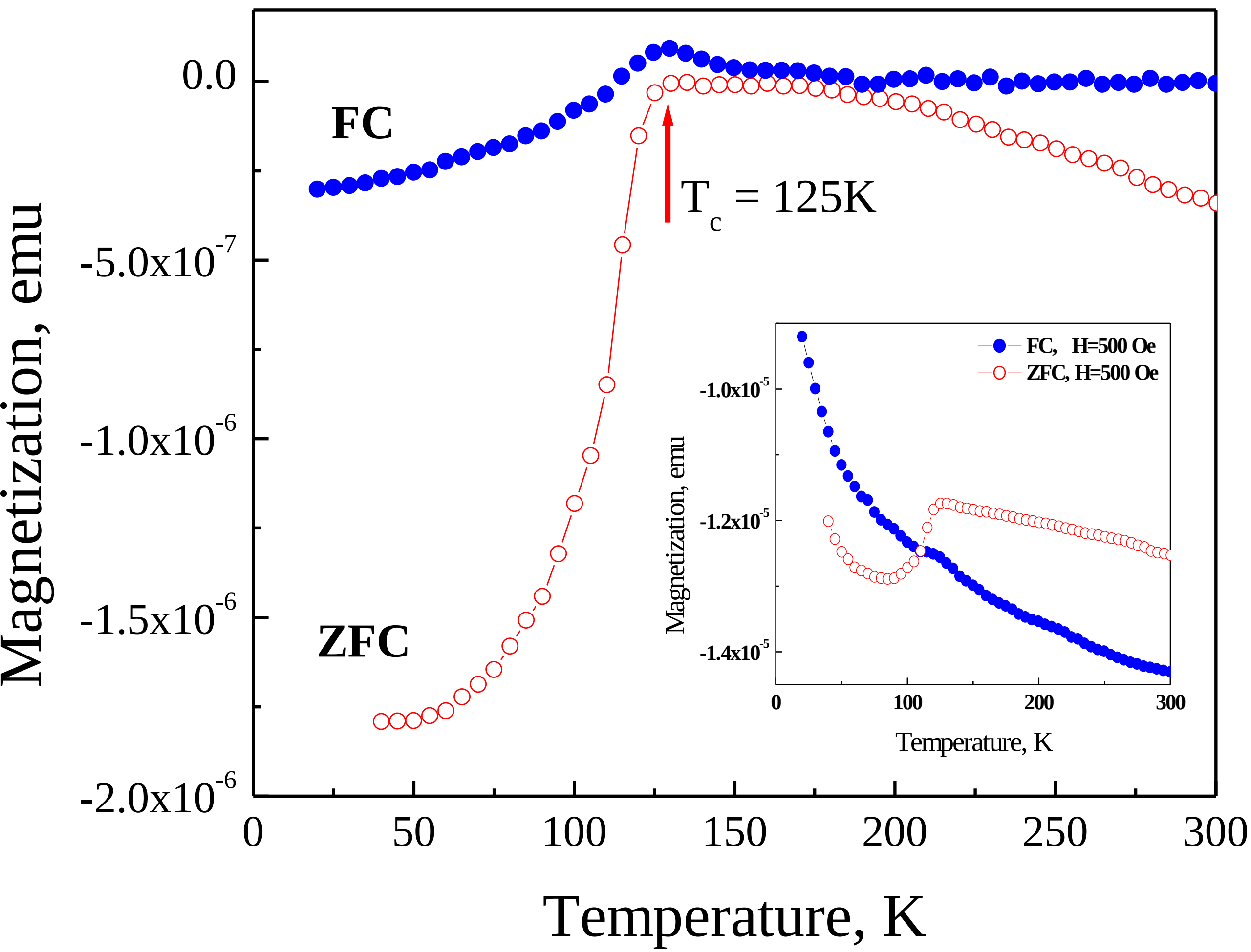

Comparison of FC and ZFC measurements in Na_xWO_{3-y} compound with subtracted paramagnetic contribution. Inset shows the measured data. Curie paramagnetic contribution was subtracted using following fitting parameters:

$M=M_o+C/T$,

$M_o=1.35x10^{-6}$ emu,

$C=12.64x10^{-6}$ emu·K.

Effect of H_2O on M(T) of NaxWO3

- Temperature dependences of magnetization measured separately in bulk WO3-y, pure carbon inverse opal matrix, carbon inverse opal infiltrated with WO3-y and last one just dipped in electrolyte without charging, do not show any diamagnetic onset in the studied range of temperatures, 50 K<T<250 K. However, we observed an intensive fluctuation in magnetization below T ~ 110 -150 K for as-prepared bulk WO3-y having high concentration of residual and physically absorbed water. Perhaps absorbed water or chemically bounded protons play an important role in formation of superconducting phase.

ZFC in Li_xWO_{3-y}: Diamagnetism at 132 K

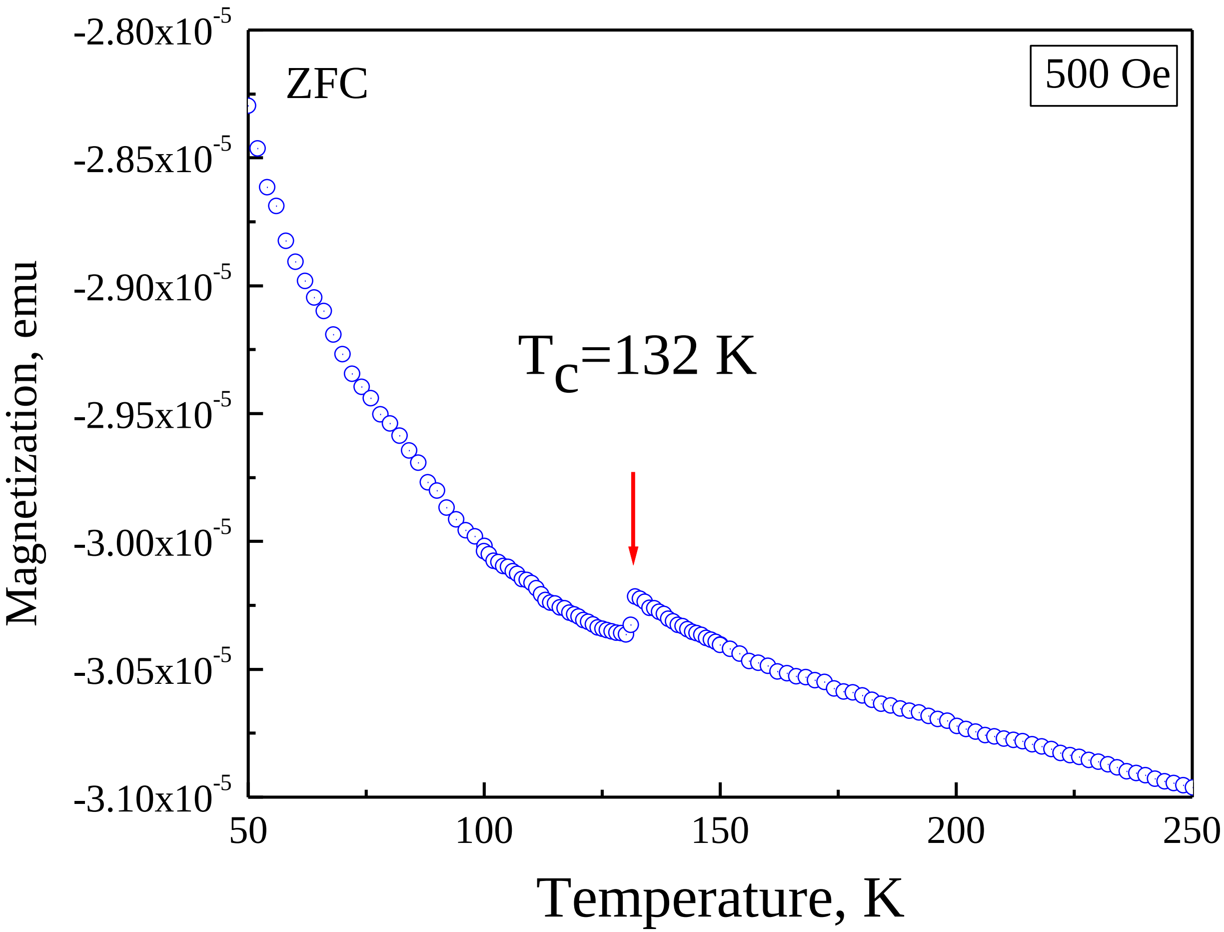

Temperature dependence of ZFC magnetization for LixWO3-y in carbon inverse opal.

Resistivity measurements drop at Tc

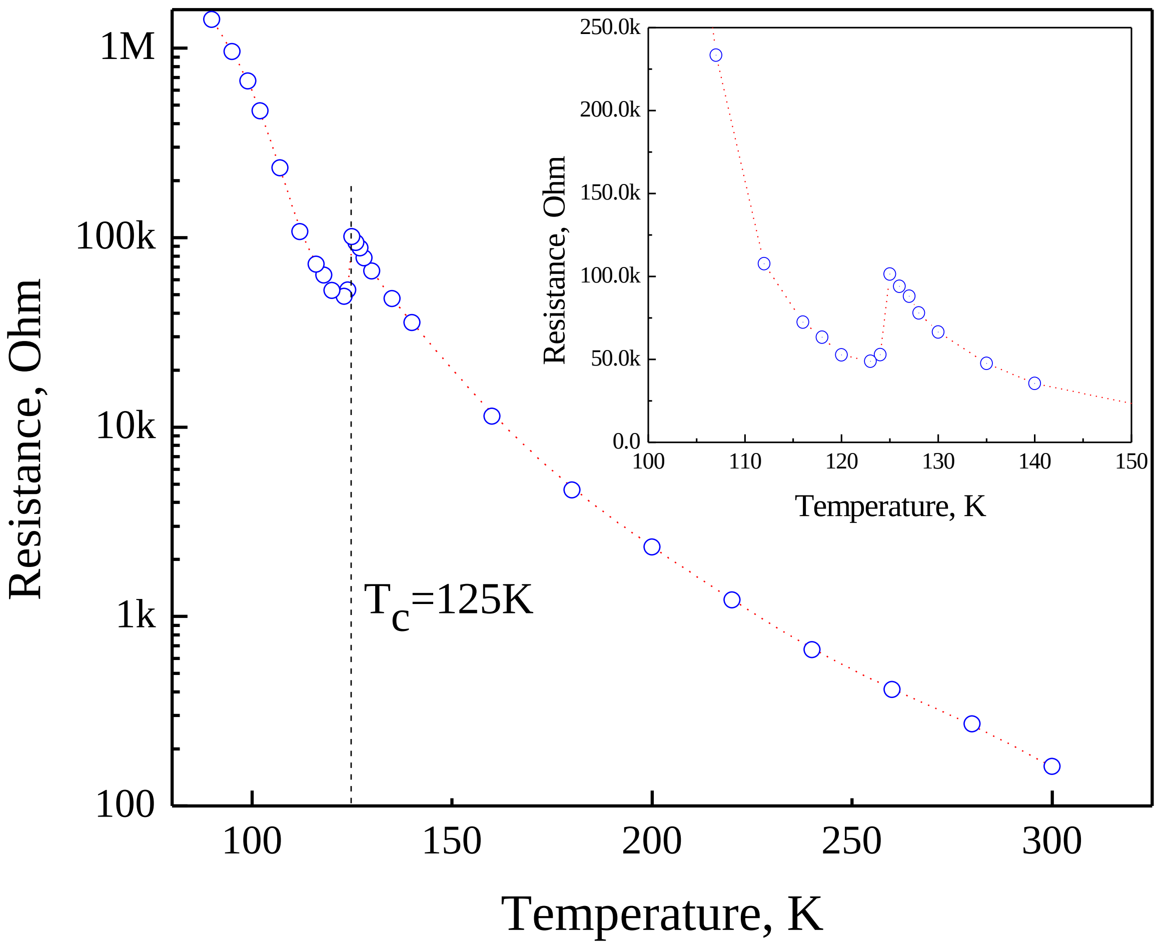

Temperature dependence of resistance in ceramic based Na_xWO_{3-y}. Applied current was 1μA.

The direct evidence of polaron formation from temperature dependence of photoemmision spectra and formation of bipolarons in weakly reduced to WO_{3-y} with 3-y typically in the order of 2.95 suggest bipolarons mechanism of a Bose-Einstein condensation of trapped electron pairs in highly doped WO_{3-x}.

Very weak and noisy LFS in $NaxWO_3$ at very low T ~ 5 K

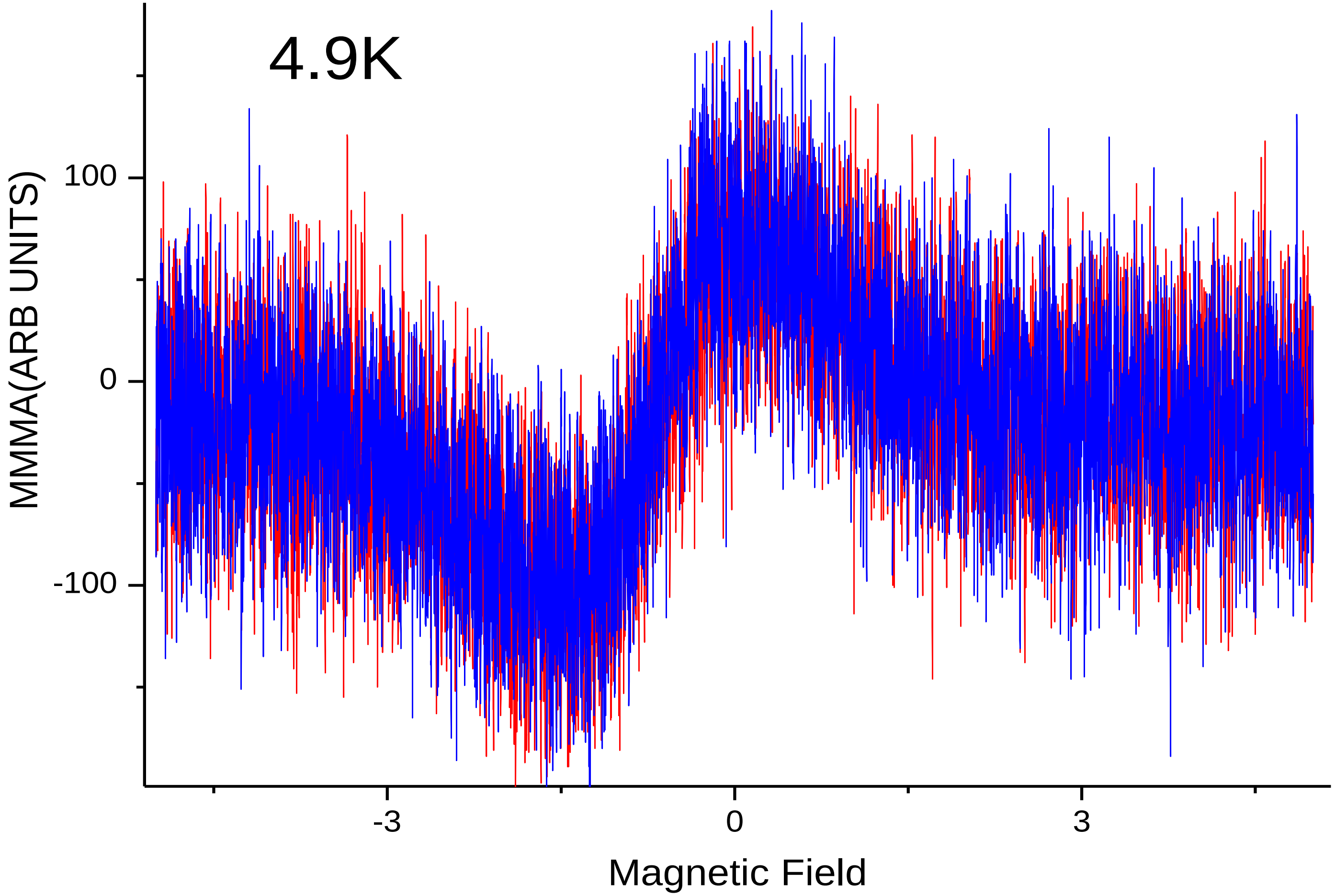

Other Nano-Matrices for NaxWO3

- As porous host matrices we tested carbon inverse opal, platinum sponge, and CVD grown multiwalled carbon nanotube paper.

- Most pronounced and reproducible onset in magnetization and resistance measurements was found for NaxWO3-y on carbon inverse opal host matrix at Tc=125 K.

Conclusion to NaxWO3

- The observed diamagnetism in ZFC and FC magnetization together with temperature behavior of resistance support the superconductive nature of obtained anomalies at Tc=125 K and Tc=132K.

- Our NaxWO3-y structures are amorphous and only samples sintered at Ts>300oC in argon atmosphere had polycrystalline structure.

- The samples sintered in argon had the deficiency of oxygen with *3-y* typically in order of 2.95.

- LFS of microwave absorption (known for type 2 SCs) is found only at very low T below, indicated different nature of superconducting phase (if any) in Na-tungsten bronze

2-D layers of HTS (or MgB_2) can be tailored into 0-D Dots, 1-D tubes or 3-D networks of inverted f.c.c.

MgB_2

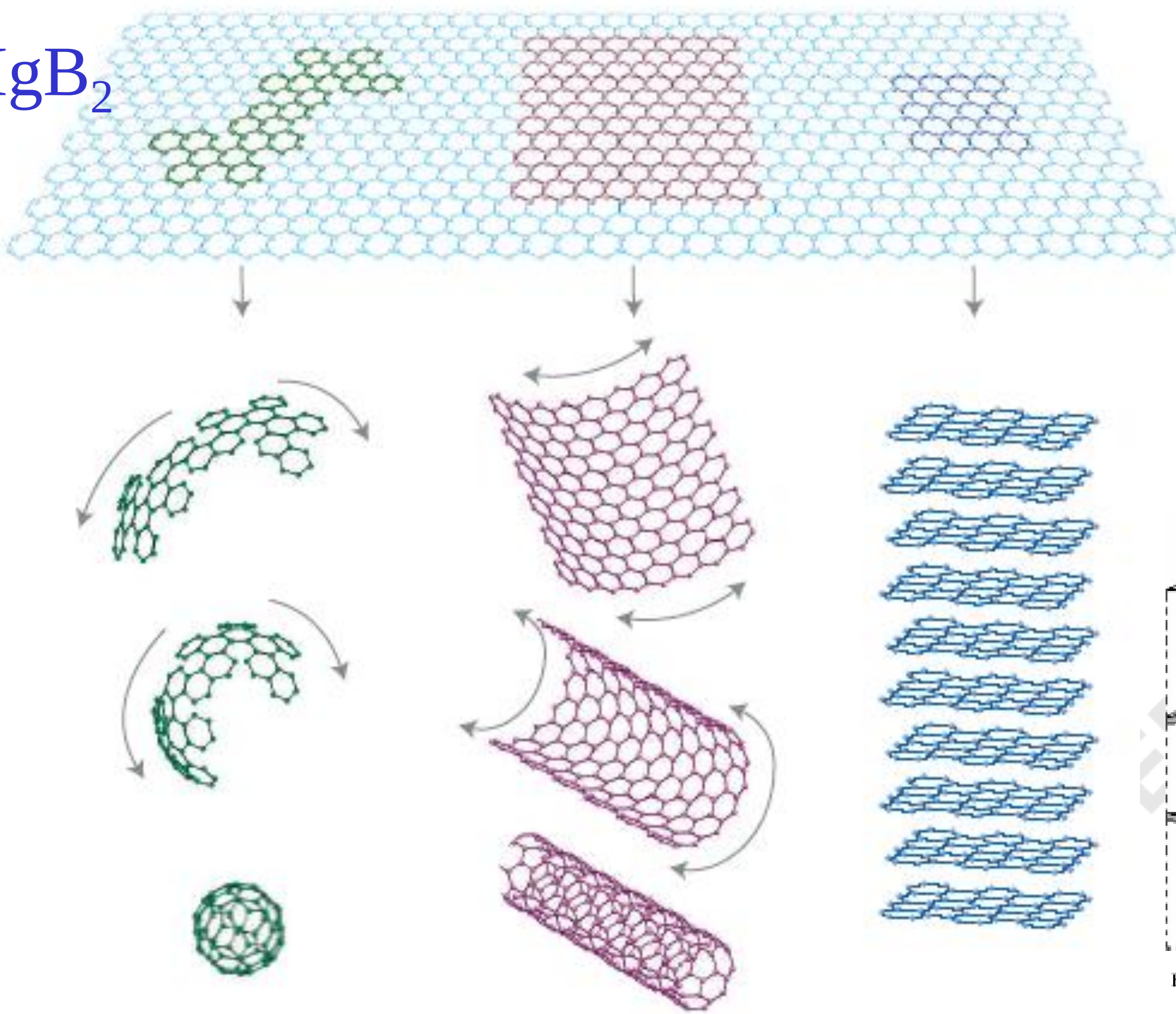

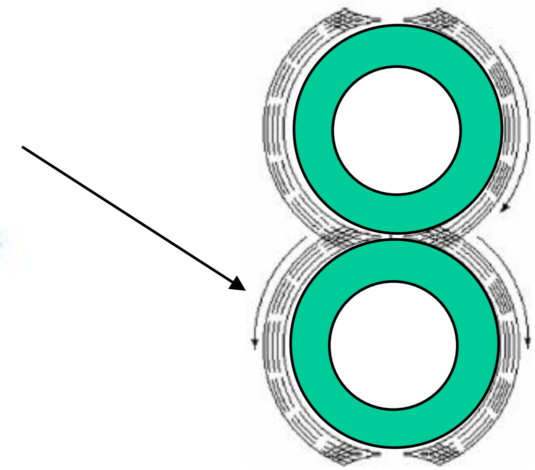

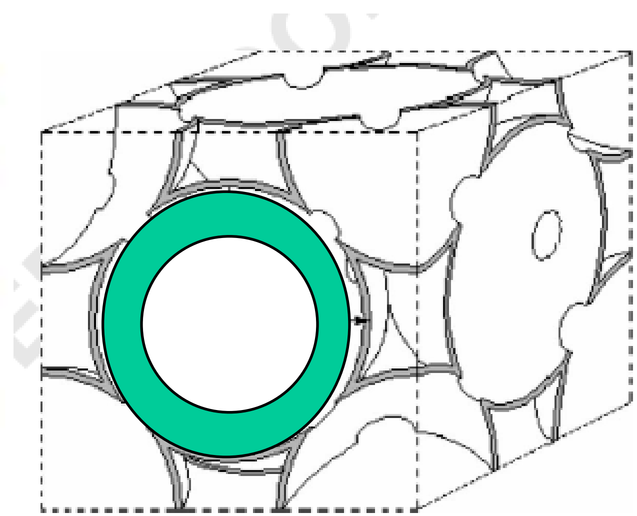

Fig. 3. Schematic representation of the surface-templated inverse opal.

Frenkel Excitons in Molecular SAM provide pairing glue

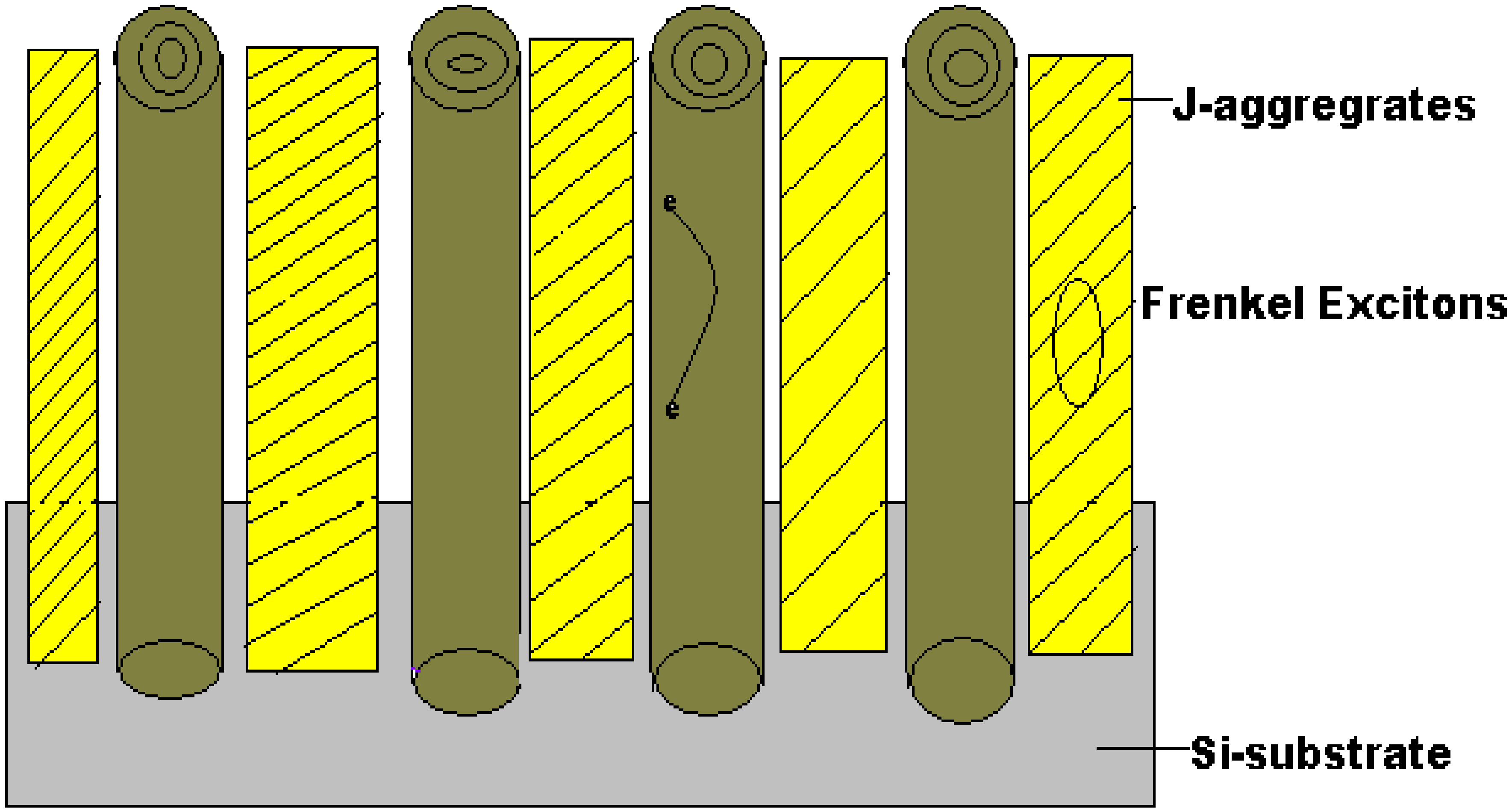

Excitons in Semiconducting Single Wall Nanotubes in bundles provide pairing glue for charges in metallic tubes

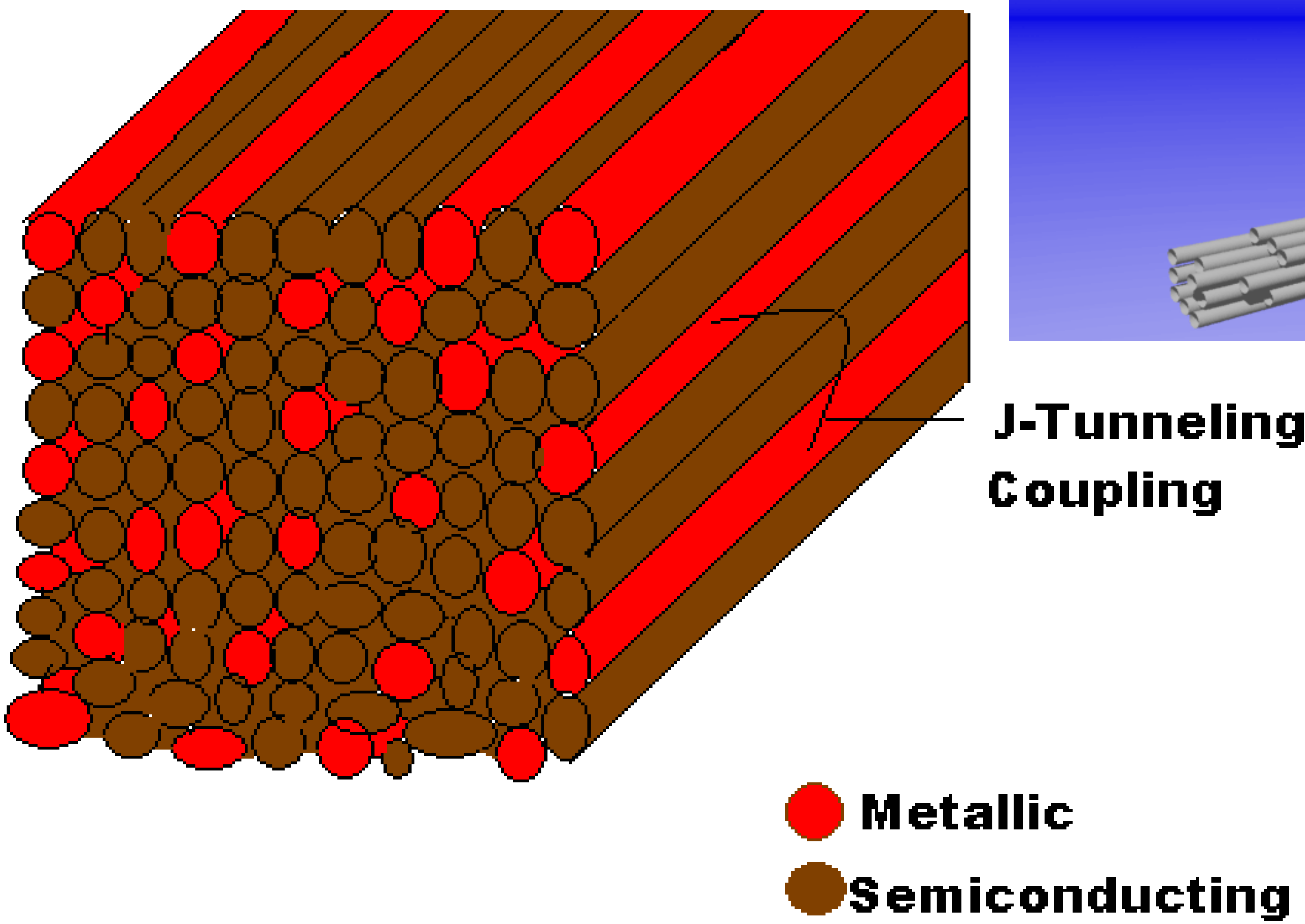

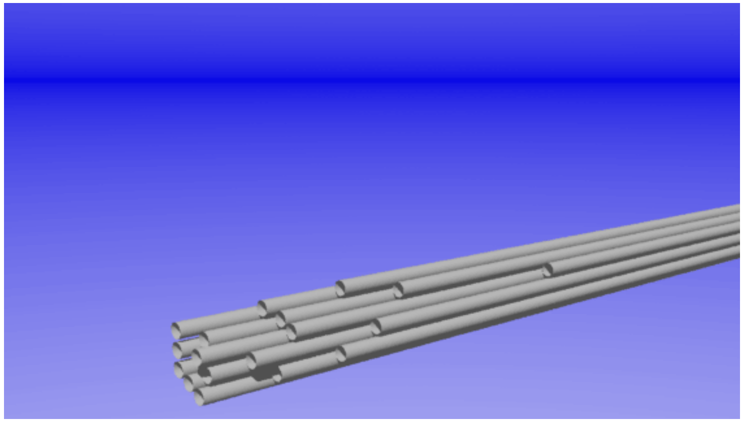

Suggestion for MgB_2 nanotubes growth

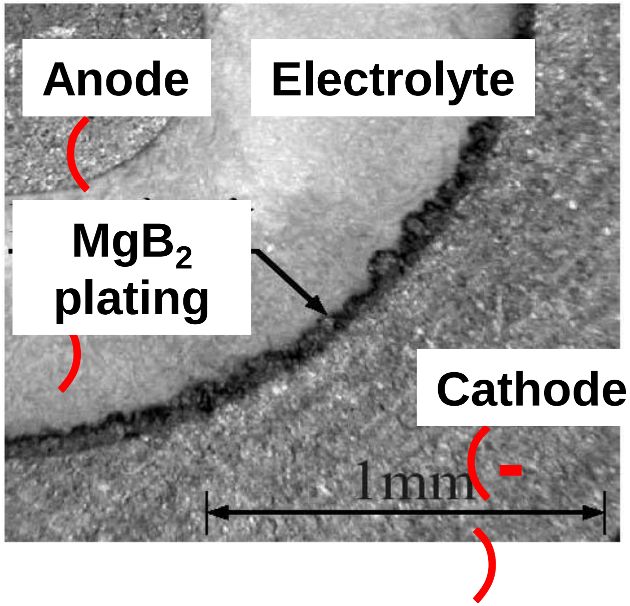

SEM image of MgB_2 thin film fabricated by Galvanization method

If highly porous carbon,
i.e. CNT forest
is used for electrode,
Then MgB2 will grow
In form of nanotubes:

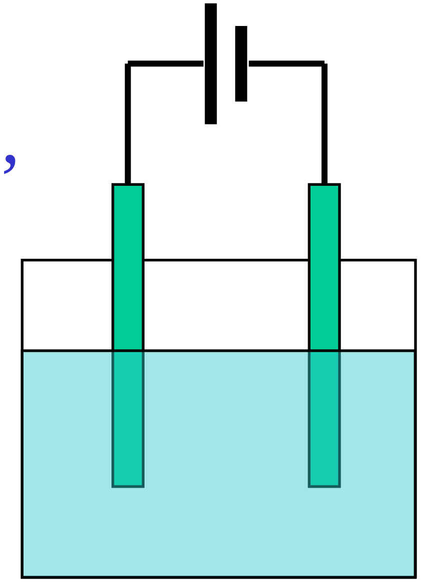

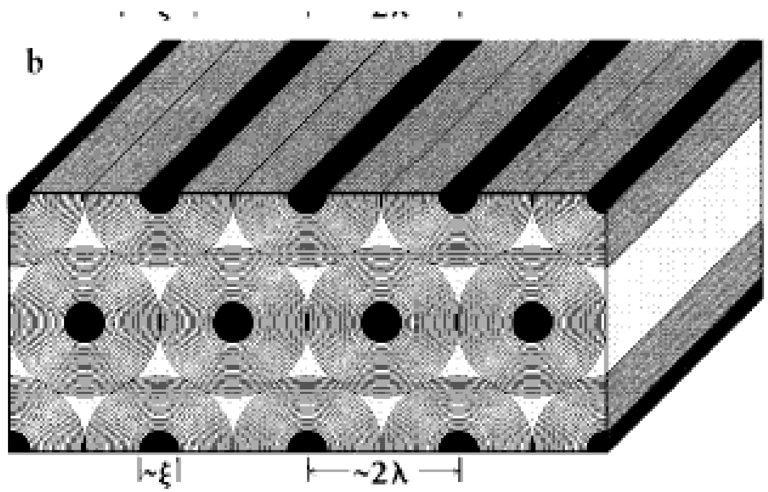

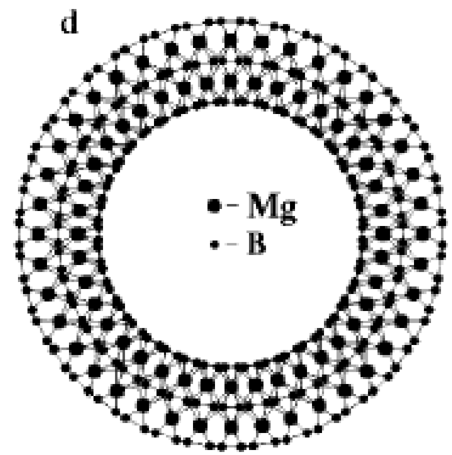

Two-walled MgB2 tubes

Perspectives for RTS

- HTS which have 2-D planes, can be converted into curved 1-D nanotubes, or into “effectively 3-D” nanosystems e.g. by electrochemical growth.

- Carrier density can be significantly increased by dry double layer doping which may increase Tc in nano-SC.

- Coating interfaces with organic dyes, will allow to study the possibility of Tc increase via Excitonic extra “pairing glue”

Ready for RTS in UTD

CNT Yarns and Sheets for RTS nanocables

Science

Vol. 306, 2004 and Vol. 309, 2005

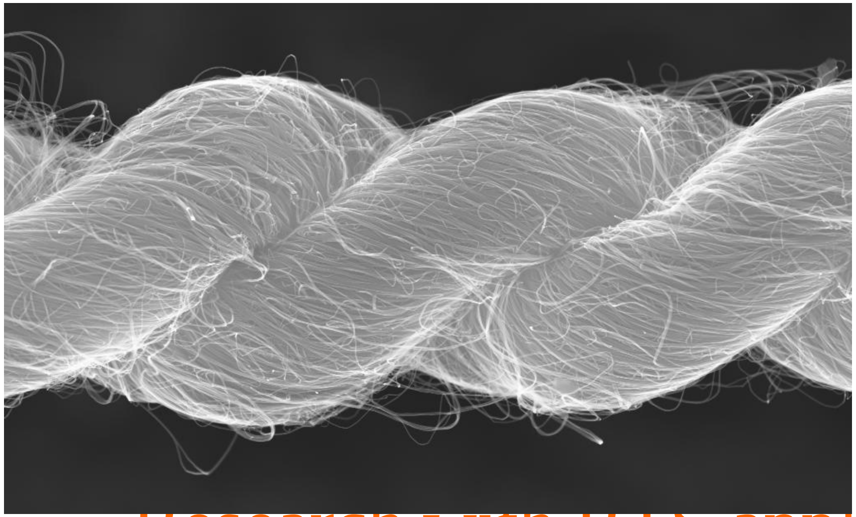

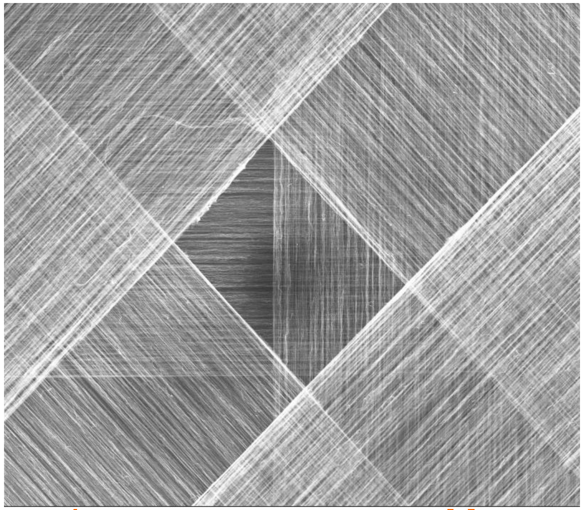

Research with RTS applications in mind!

"Science is People!"

Alan MacDiarmid, 2000 Nobel laureate in Chemistry

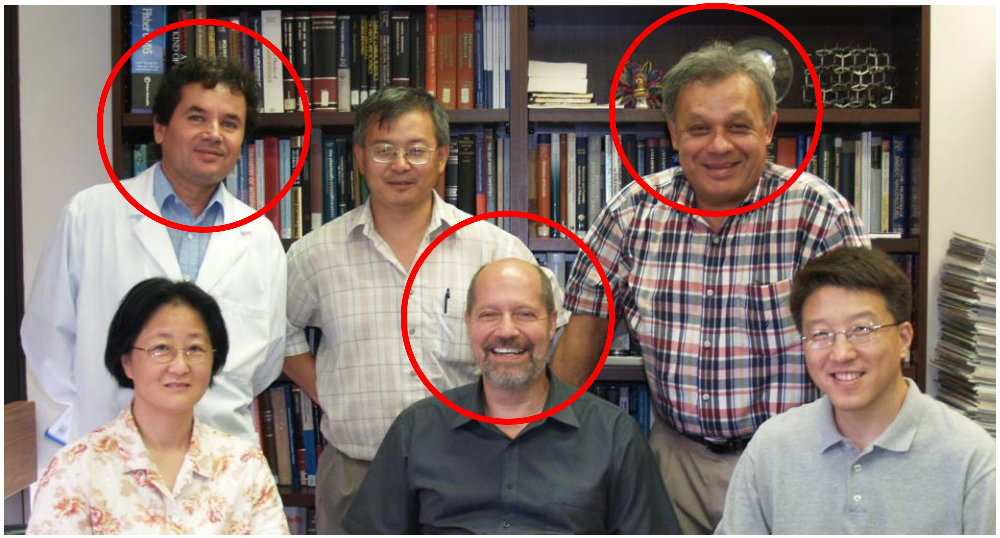

UTD Superconductivity Team:

Ali Aliev,
Anvar Zakhidov,
Ray Baughman

Funding

- US Air Force via AFOSR programs
- Robert A. Welch Foundation
- Defense Advanced Research Projects Agency
- SPRING (Strategic Partnership for Research in Nanotechnology)

Excitons in Quantum Dots provide pairing glue in metallic single wall carbon nanotubes

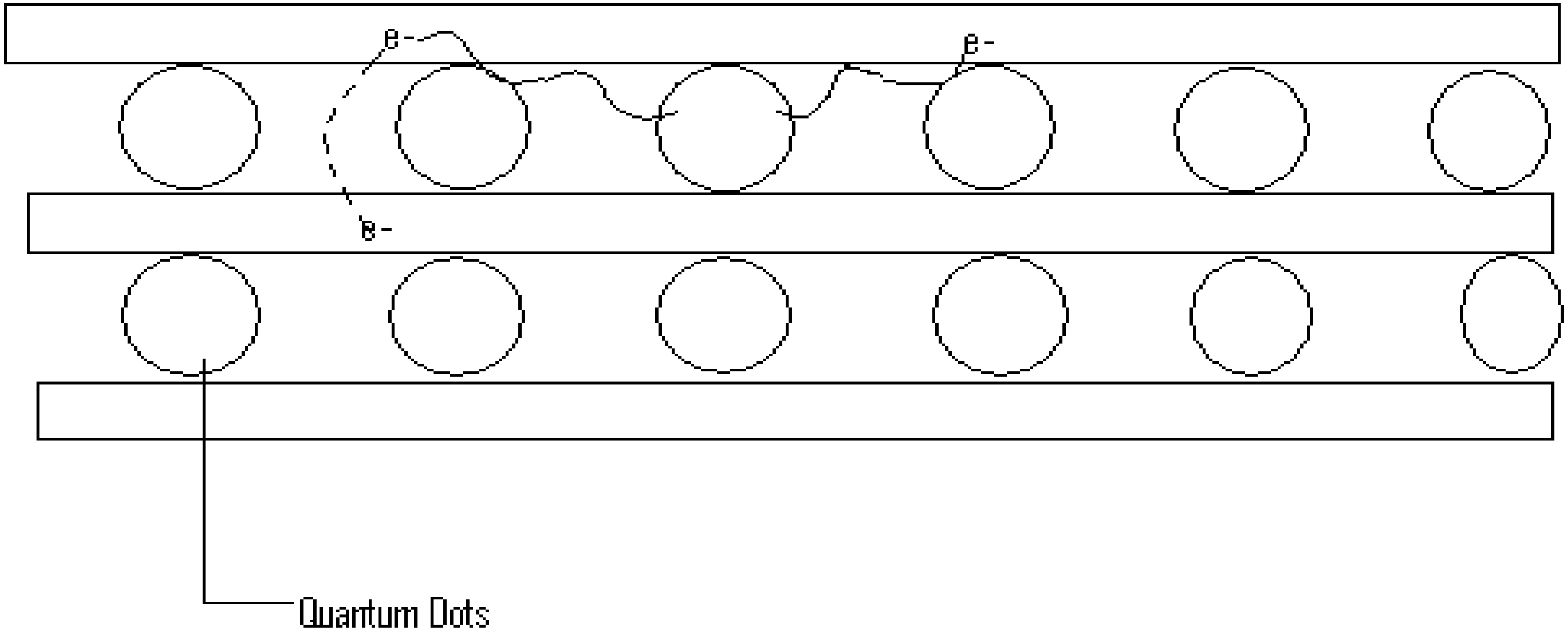

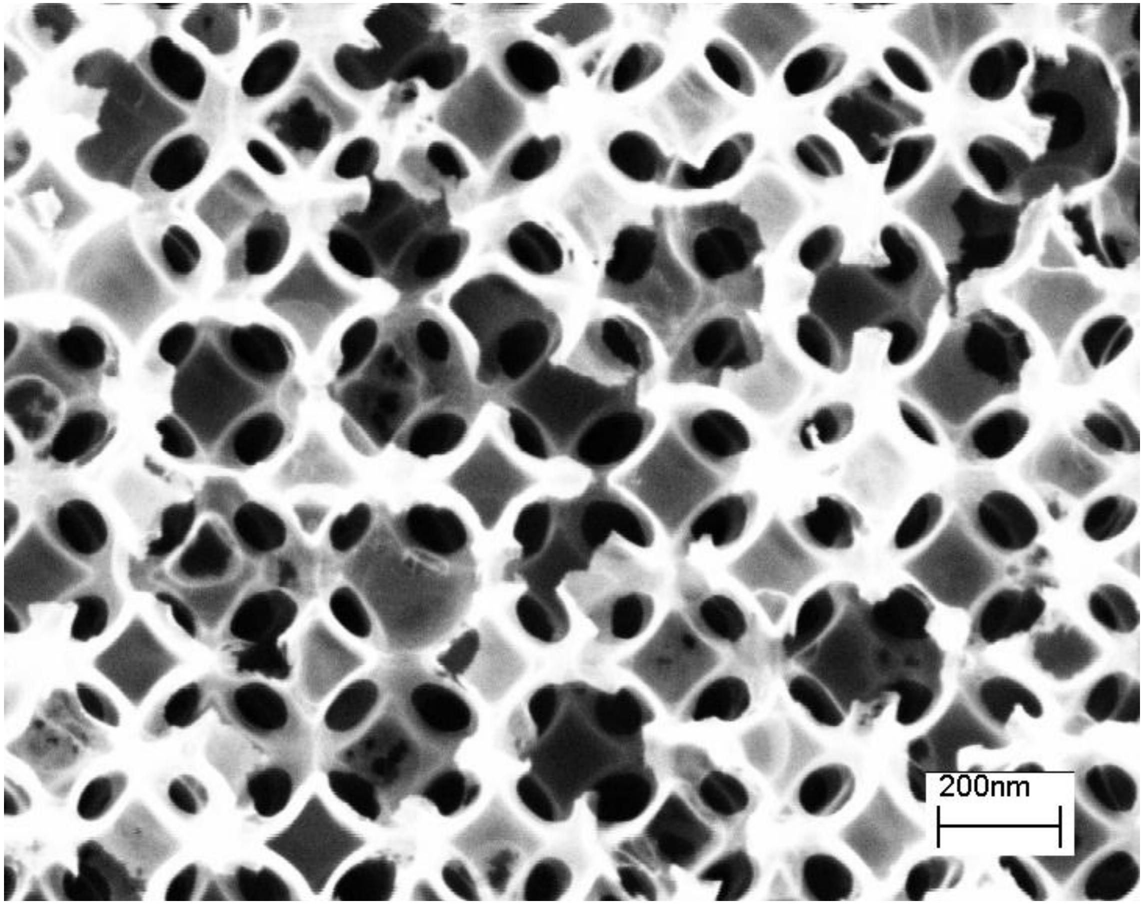

Fig. 8

Nanostructured superconductors: from granular through wire towards high-T_c nanotubular 2D composites

Vladimir Pokropivny

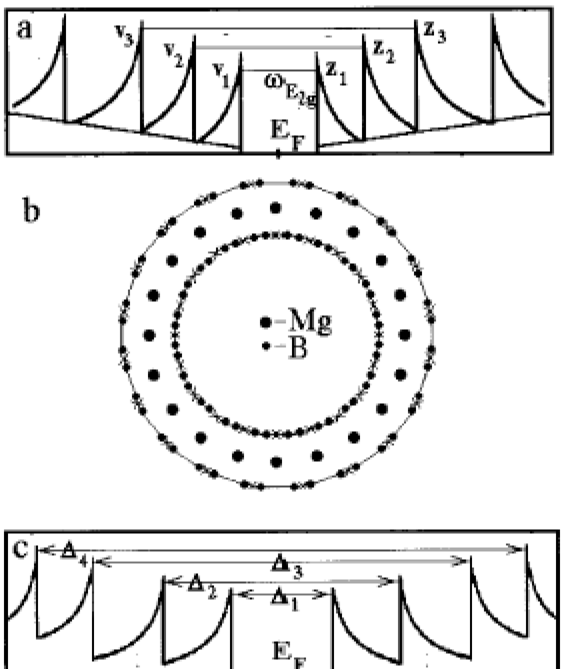

Figure 3 Two kinds of ideal high-T_c-superconductors on base of membrane 2D crystals (a lattice parameter of which is about the double penetration depth of a magnetic field $a \sim 2\lambda$), built from nanotubes (diameter of which is about the correlation length $d \sim \xi$), wrapped from layered superconducting materials: (a) square lattice of nanotubes deposited on inner walls of nanocylinders of 2D-membrane; (b) triangle lattice of nanotubes deposited on outer walls of nanofibers of 2D brush-like lattice; (c) cross-section of the single-walled LuNiBC nanotube; (d) cross-section of the two-walled MgB_2 nanotube

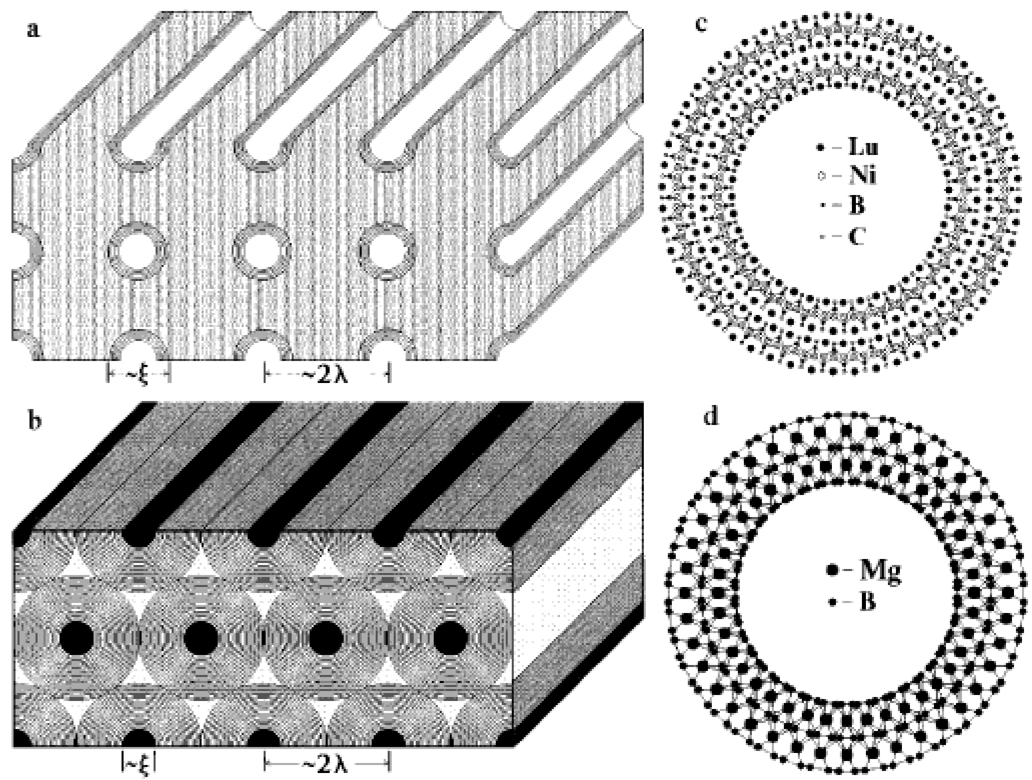

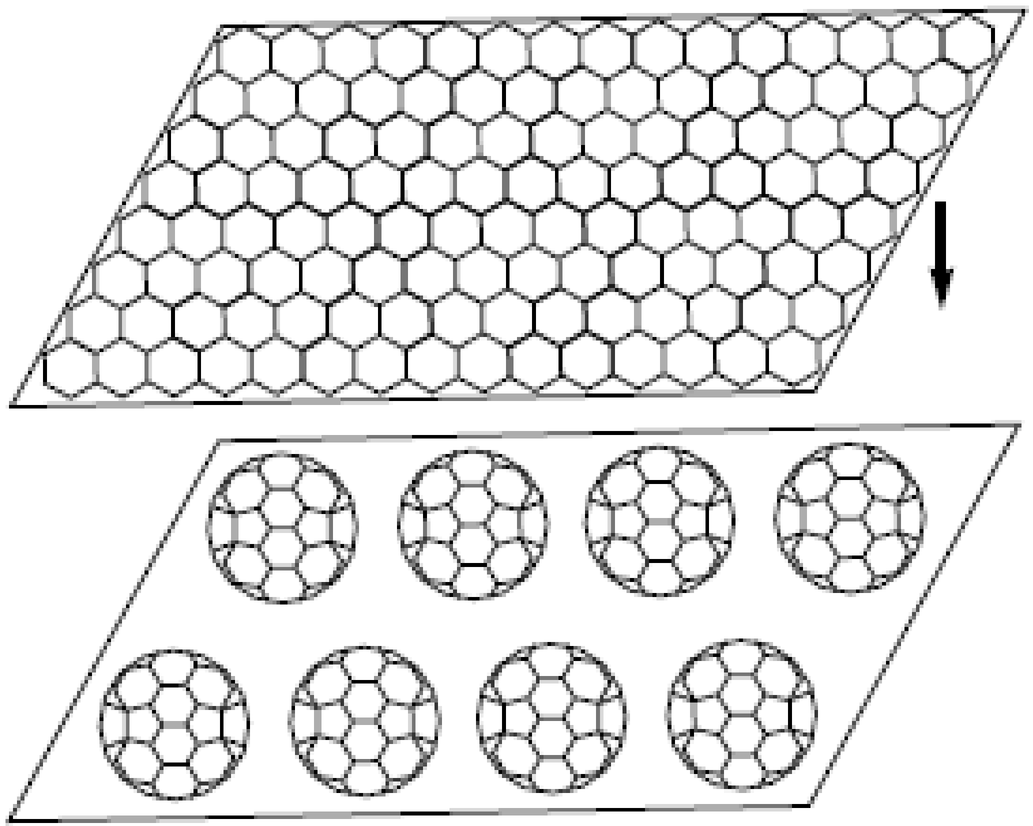

Figure 10.7. Intercalation of graphene sheets by C_{60} molecules.

- In addition to experiments on single crystals of pure or polymerized fullerenes,

the fullerenes can also be used in a combination with graphite or/and nanotubes. One can intercala te the graphene sheets in graphite by fullerenes

Possible explanation of Tc> 100 K

An explanation of such enhancements of T_c was proposed, twenty five years ago, by Lefkowitz,[19] who thought that the anomalous $T_c(x)$ dependence in the tungsten bronzes was a surface effect: he stressed that a ferroelectric instability can condense at low temperatures in WO_3 and hypothesized that this could lead to high electric fields at the boundary between the insulating material and the doped regions—thus inducing a new electron density of states at the

Fermi level. Although we are now quite sure that the increase in T_c with the reduction of the alkali content in these bronzes is really a bulk property, the Lefkowitz's proposition seems fairly seductive when considering the phenomenon we observed in the vapor-transported samples.

[19] I. Lefkowitz, Ferroelectrics 16, 239 (1977).

Inspired by Vitaly Ginzburg, my grand-teacher and the leader of Russian program on High Tc

Vitaly Ginzburg and Vladimir Agranovich
“Krasnaya Polyana”, Chehov, 2004